Resistant tomato restricts colonization and invasion by the pathogen *Ralstonia solanacearum* at four organismal levels

Marc Planas-Marquès[1,±], Jonathan P. Kressin[2,3a,¥,±], Anurag Kashyap[1], Dilip R. Panthee[3a], Frank J. Louws[2,3b], Nuria S. Coll[1,*,✉], Marc Valls[1,4,*,✉]

1 Centre for Research in Agricultural Genomics (CRAG), CSIC-IRTA-UAB-UB, Campus UAB, Bellaterra, 08193 Barcelona, Catalonia, Spain.
2 Department of Entomology and Plant Pathology, North Carolina State University, Raleigh, NC 27695, USA.
3 Department of Horticultural Science, North Carolina State University, [a]Mountain Horticultural Crops Research and Extension Center, Mills River, NC 28759, USA and [b]Raleigh, NC, 27695.
4 Department of Genetics, University of Barcelona, 08028 Barcelona, Catalonia, Spain.
[±] MPM and JPK should be considered joint first authors.
* NSC and MV should be considered joint senior authors.
¥ Current address: Department of Breeding, Hortigenetics Research (S.E.Asia) Ltd., East-West Seed Co., Chiang Mai, Thailand 50290

✉ To whom correspondence should be addressed: Nuria S. Coll (nuria.sanchezcoll@cragenomica.es) and Marc Valls (marcvalls@ub.edu). Phone number: +34 5636600

E-mail addresses:
Marc Planas-Marquès: marc.planas@cragenomica.es
Jonathan P. Kressin: jpkressi@gmail.com
Anurag Kashyap: anurag.kashyap@cragenomica.es
Dilip R. Panthee: dilip_panthee@ncsu.edu
Frank J. Louws: frank_louws@ncsu.edu
Nuria S. Coll: nuria.sanchezcoll@cragenomica.es
Marc Valls: marcvalls@ub.edu

Running title: Restriction of *R. solanacearum* colonization in resistant tomato

Date of submission: 4th of September 2019

Word count (from Introduction to Acknowledgements): 6465

Number of figures: 8 (Figure 6 and 7 to be published in color in print),
Supplementary data: 9 figures as supporting Information.

Highlight

We show the spatio-temporal dynamics of the tomato-*Ralstonia solanacearum* interaction, revealing an out-of-the-xylem spread. We set the foundations to study the complex molecular mechanisms that control each restriction point.

Abstract

Ralstonia solanacearum is a devastating bacterial vascular pathogen causing bacterial wilt. In the field, resistance against this disease is quantitative and only available for breeders in tomato and eggplant. To understand the basis of resistance in tomato, we have investigated the spatio-temporal bacterial colonization dynamics using non-invasive live monitoring techniques coupled to grafting of susceptible and resistant varieties. We revealed four different restrictions to the bacterium in resistant tomato: root colonization, vertical movement from roots to shoots, circular vascular bundle invasion and radial apoplastic spread in the cortex. We also show that the radial invasion of cortical extracellular spaces occurs mostly at late disease stages but is observed throughout plant infection. This work shows that resistance is expressed both in root and shoot tissues and highlights the importance of structural constraints to bacterial spread as a resistance mechanism. It also shows that *R. solanacearum* is not only a vascular pathogen but spreads “out of the xylem”, occupying the plant apoplast

niche. Our work will help elucidate the complex genetic determinants of resistance, setting the foundations to decipher the molecular mechanisms that limit pathogen colonization, which may provide new potential precision tools to fight bacterial wilt in the field.

Keywords: bacterial wilt, disease resistance, *Ralstonia solanacearum*, tomato, vascular pathogen, xylem

INTRODUCTION

Bacterial wilt caused by the *Ralstonia solanacearum* species-complex is a disease of major economic importance, impacting production of solanaceous crops, legumes, banana, ginger and ornamentals (Hayward, 1994). *R. solanacearum* enters the roots through wounds, colonizes the xylem tissue, moves up into the stem and causes a rapid, permanent wilt through a combination of high bacterial densities and mass-production of extracellular polysaccharides (Hayward, 1991; Grimault and Prior, 1993; McGarvey *et al.*, 1999; Schell, 2000). *R. solanacearum* can move across the root following either an apoplastic pathway through the middle lamella or a pseudo-symplastic pathway via the xylem vessel lumens and axillary pits (Schell, 2000).

Management of bacterial wilt remains challenging due to *R. solanacearum* aggressiveness, its broad geographical distribution, wide host range, and long persistence in soil and water (Genin, 2010; Mansfield *et al.*, 2012). Strong quantitative resistance to bacterial wilt in tomato has been available for many decades, but has only been successfully deployed in small-fruited varieties (<200 g) and rootstocks for grafting due to a seemingly unbreakable linkage between small fruit size and resistance (Scott *et al.*, 2005; Rivard and Louws, 2008). The Hawaii breeding line series, particularly Hawaii 7996, is the most effective source of resistance against various *R. solanacearum* strains under different environmental conditions and are widely used rootstocks for bacterial wilt management (Grimault *et al.*, 1994*a*; Prior *et al.*, 1996; Wang *et al.*, 1998).

‘Shield’ is a commercially successful hybrid that has been the most planted rootstock for bacterial wilt resistance in North Carolina in the past years, behaving in this location as highly resistant in fields with moderate disease pressure (Suchoff *et al.*, 2015), but showing an intermediate resistance level under strong disease pressure (Kressin *et al.*, unpublished). Resistance in a mapping population derived from Hawaii 7996 (resistant) x West Virginia 700 (susceptible) has been reported to be mainly quantitative, involving two major Quantitative Trait Loci (QTLs) located in chromosomes 12 and 6 (Bwr-12 and Bwr-6), accounting for 18-56% and 11-22% of the phenotypic variation, respectively (Wang *et al.*, 2013), and three minor loci (Bwr-3, Bwr-4 and Bwr-8). Some of these QTLs are strain- and/or environment-specific (Carmeille *et al.*, 2006; Mangin *et al.*, 1999; Thoquet *et al.*, 1996*a*; Thoquet *et al.*, 1996*b*; Wang *et al.*, 2000; Wang *et al*., 2013).

Initial studies on *R. solanacearum* colonization in several resistant and susceptible tomato varieties described that bacterial wilt resistance was associated with the capability of the plant to limit bacterial spread from the root collar to the midstem and not with limited root invasion (Grimault and Prior, 1993; Nakaho, 1997*a*). However, when similar experiments were repeated without wounding the roots, limited bacterial growth in Hawaii 7996 was observed in all tissues analyzed: taproot, hypocotyl, petiole and mid-stem (McGarvey *et al.*, 1999).

Studies analyzing plant colonization in grafted tomatoes showed that the bacterium was capable of crossing the graft junction into the susceptible scion. Hawaii 7996 rootstocks were the most efficient in limiting susceptible scion infection to 38% and wilting to only 10% in conditions where susceptible varieties were 100% infected and wilted (Nakaho *et al.*, 2004).

Microscopic observation of tomato bacterial wilt described the presence of inducible physico-chemical barriers (tyloses, gums and modifications to the primary cell wall) that seemed to limit bacterial spread in the Caraïbo resistant variety (Grimault *et al.*, 1994*b*). Light microscopy studies of upper hypocotyls revealed that bacterial masses were present only in the primary xylem tissues in resistant LS-89 plants (derived from the Hawaii line 7998), whereas bacteria were found in both the primary and secondary xylem tissues of susceptible Ponderosa (Nakaho, 1997*a*). Thus, disease severity in *R.*

solanacearum-infected tomato plants was proposed to correlate with the extent of bacterial invasion into the secondary xylem tissues (Nakaho, 1997*a*,*b*). This limitation of pathogen movement from the protoxylem or the primary xylem to other xylem tissues was found most conspicuous in Hawaii 7996 (Nakaho *et al.*, 2004). Other studies described that cell walls were thicker in parenchyma and vessel cells of infected xylem tissues in the resistant LS-89 than in susceptible Ponderosa or mock-inoculated plants (Nakaho *et al.*, 2000). Accumulations of electron-dense materials in vessels and parenchyma cells were also described as more apparent in LS-89, while Ponderosa showed necrosis in all parenchyma cells adjacent to vessels with bacteria (Nakaho *et al.*, 2000). A recent report microscopically studied *R. solanacearum* distribution in roots of Hawaii 7996 and the susceptible cultivar West Virginia 700 and found that colonization of the root vascular cylinder was delayed and movement inside the vasculature was spatially restricted in Hawaii 7996 (Caldwell *et al.*, 2017).

Together, these studies underscore the existence of a complex set of events that restrict bacterial colonization in space and time in resistant varieties. However, a systematic investigation of *R. solanacearum* invasion patterns at a whole plant and tissue-system level is lacking.

Here, we have applied luminescent and fluorescent bacteria for the characterization of bacterial wilt resistance in tomato root, hypocotyl, and stem organs at the tissular level. We have compared highly susceptible, moderately resistant, and highly resistant grafted tomato plants using a standard soil-based seedling grafting method and an *in vitro* grafting method. We propose an integrative model for bacterial wilt in resistant tomato lines that highlights the importance of four different restriction levels that limit bacterial colonization: 1) Invasion of the root 2) vertical movement upwards to the stem, 3) circular passage from vessel to vessel and 4) xylem escape and radial spread into the pith/cortex tissues.

MATERIALS AND METHODS

Plant and bacterial materials and growth conditions

The tomato (*Solanum lycopersium)* lines used in this study were the highly susceptible commercial variety ‘Marmande’ (Leroy Merlin), the moderately resistant commercial

hybrid rootstock ‘Shield’ (Rijk Zwaan), and the highly resistant public open-pollinated breeding line ‘Hawaii 7996’.

For *in vitro* experiments, tomato seeds were surface sterilized in 35% bleach and 0.02% Triton-X 100 for 10 minutes and rinsed with sterile distilled water 5 times before sowing them on semi-solid medium (Murashige and Skoog, MS, with agar) in square culture plates (Sudelab S.L.). Plates were placed standing upright in a walk-in tissue culture growth chamber set at 22ºC under long day light conditions.

For pot experiments, plants were grown on soil (Substrate 2, Klasmann-Deilmann GmbH) mixed with perlite and vermiculite (30:1:1) in a growth chamber (either a FITOCLIMA 1200, Aralab, or a SCLAB S.L., set at 27^{o}C or 25^{o}C, respectively) with 60% humidity under 12h day/night LED or fluorescence lighting (light intensity of 120-150 µmol·m^{-2}·s^{-1}), respectively.

All assays were performed using *Ralstonia solanacearum* GMI1000 strain. The constructs PpsbA::LuxCDABE and PpsbA::GFPuv generated by Cruz *et al*. (2014) were naturally transformed into *R. solanacearum* GMI1000 to generate the reporter strains. *R. solanacearum* was grown as previously described (Planas-Marquès *et al.*, 2018).

Plant grafting

For *in vitro* grafting, seeds were sown onto sterile filter paper placed on MS-containing plates. Eight days after germination (seven for Marmande to obtain equivalent stem diameters), cotyledons were removed and the plants were cut at a perpendicular angle 1 to 2 cm below the cotyledons using sterile tools. For double grafted plants, two 2 to 3 cm-distant-cuts were performed. Rootstocks and scions were transferred to fresh plates without filter paper and matched with the corresponding reciprocal tissues without any stabilizing device. Plates were kept standing upright in the growth chamber. After 10 days, successfully healed plants were either pin-inoculated with the luminescent strain and monitored over time or transferred to soil-containing pots and grown as described for pathogenicity assays after acclimation for 48h in transparent boxes (Altuna 2594005, Stewart Garden) with vented lids opened after 24h.

For standard grafting, plants grown with stems 1.5-2 mm in diameter (9 days after sowing) were grafted 2 cm below the cotyledons using a 70º angle cut and 1.6 or 2 mm

diameter grafting clips (Bato Plastics B.V). Grafted plants were kept into misted acclimation boxes in growth chambers and acclimated to light (24h darkness, 24h at 10% light, 24h at 50% light) and then to ambient humidity (opening the vents 4 days after grafting and partly opening the lid for 48h before removing it).

Plant inoculation and pathogenicity assays

For *in vitro* assays, 10 day old plantlets or plantlets 10 days after grafting were pin-inoculated 1 cm below the root collar using a sterile 0.3x13mm-sized needle (30Gx½, BD Microlance, Becton Dickinson) submerged in a 10^6 CFU·ml^{-1} (OD_{600}=0.001) *R. solanacearum* suspension. Plates were kept in growth chamber (25ºC day, 22ºC night) and wilting symptoms recorded and bacterial invasion visualized as detailed below.

For soil drenching inoculations, plants were grown until they reached between the 7 and 9 true leaf stage (4 to 5 weeks after sowing, and 5 to 6 weeks for grafted plants). Inoculations were performed by pouring 40 ml of 10^7 CFU·ml^{-1} (OD_{600}=0.01) of bacterial suspension on every pot after making four holes in the soil with a disposable 1-ml pipette tip. Plants were scored for wilting symptoms using a 0 to 4 scale, where 0 = healthy plant, no wilt; 1 = 25%, 2 = 50%, 3 = 75% and 4 = 100% of canopy wilted. To assess shoot colonization, 4 to 5 week-old plants were pin-inoculated with 10 µl of 10^6 CFU·ml^{-1} (Ishihara *et al.*, 2012) when indicated.

Assessment of bacterial invasion

R. solanacearum invasion was assessed using luminescent and fluorescent strains. For *in vitro* assays, pin-inoculated plants were photographed using light imaging (ChemiDoc Touch Imaging System, Bio-Rad) as previously described (Cruz *et al.*, 2014) using a 5-minute exposure time with the 3x3 sensitivity. Images were processed using the Image Lab software (Bio-Rad). Inoculated soil-grown plants were uprooted, roots were surface-sterilized in water with ~5 to 10% bleach for at least 1 minute followed by a wash in water. Plants inoculated with the luminescent strain were sliced from apex to roots using a sterile razor blade. One mm-thick transverse sections and the two halves of 1 to 2 cm-length radial slices were placed flat on a square plate with a misted lid and visualized using live imaging system as detailed before. For each location, a 0.5 cm

section was excised and incubated for at least 30 minutes into a sterile 2 ml tube with 200 µl of sterile distilled water. Luminescence was measured on a luminometer (FB 12, Berthold Detection Systems). Relative Light Units per second ($RLU \cdot s^{-1}$) were related to Colony Forming Units per gram of tissue ($CFU \cdot g^{-1}$) after dilution plating of samples and CFU counting 24h later.

Plants inoculated with the fluorescent strain were dissected as before and photographed using binocular microscopy with a UV fluorescent lamp (BP330-385 BA420 filter) and DP71 camera system-equipped SZX16 Stereo microscope (Olympus). Quantification of mean fluorescence in the green, blue and red channels was achieved using the ImageJ software.

Statistical analysis

Statistical analyses were performed using the Statgraphics software. All tests are indicated on the respective figure legends.

RESULTS

The first bottleneck in *R. solanacearum* colonization: the root-to-shoot boundary

Limited shoot colonization in resistant tomatoes has been proposed to be due to reduced *R. solanacearum* spread from the root to the stem (Grimault and Prior, 1993; Nakaho, 1997*a*) and/or limited root invasion in resistant varieties (McGarvey *et al.*, 1999; Caldwell *et al.*, 2017). To clearly define at what level(s) of the plant was resistance acting, we took advantage of a constitutively luminescent *R. solanacearum* that we had previously generated (Cruz *et al.*, 2014) to follow in a non-disruptive manner bacterial colonization in resistant and susceptible tomato plants. For this, we established a miniaturized in vitro tomato-*R. solanacearum* infection system. Tomato seedlings were grown on semi-solid medium and pin-inoculated at the root level with the luminescent strain. Forced inoculation ensured infection of all plants to study bacterial spread in the plant tissues. Disease symptoms were recorded as the percentage of wilted plants (Fig. 1A) and plants were photographed using live imaging over time. This

non-destructive assay mimicked the disease symptomatology observed in field or greenhouse conditions under strong disease pressure, as indicated by the reduced wilting of the resistant line Hawaii (H7996) compared to the susceptible Marmande (Fig. 1A). While all tomato roots were colonized 3 days post inoculation (dpi) (Fig. 1B left panel), shoot colonization was clearly delayed and reduced in H7996 compared to Marmande as indicated by the percentage of plants in which bacterial colonization was detected (Fig. 1B right panel). A representative photograph of the assay at 4 dpi, when the susceptible plants start to wilt, is presented in Figure 1C. This image shows that, besides the described difference in shoot colonization in both varieties, a colonization bottleneck exists in resistant plants at the level of the root collar. In addition, luminescence levels were lower in the roots of H7996 (Fig. 1C), indicating lower bacterial loads compared to Marmande plants.

Resistant rootstocks reduce plant invasion and limit bacterial multiplication in the roots of grafted plants

To analyze the contribution of the root to resistance in further detail, we grafted rootstocks and scions of Marmande and H7996. Grafts were made at the upper hypocotyl and at the root collar levels, and bacterial colonization and disease progression were evaluated using the luminescent *R. solanacearum* strain after root pin-inoculation (Fig. 2). Resistant H7996 rootstocks hampered bacterial colonization of Marmande shoots, while Marmande roots did not prevent colonization of the H7996 scions (Fig. 2A). Interestingly, the presence of a resistant root system was sufficient to cause a reduction in shoot colonization, as stem luminescence was comparable in grafted plants with or without a resistant lower stem (Fig. 2B).

To strengthen the previous observations, we investigated *R. solanacearum* root colonization in fully developed plants inoculated by soil drenching with the luminescent *R. solanacearum* strain. The tomato variety Shield, which is moderately resistant to bacterial wilt, was introduced in these experiments for comparison with the susceptible Marmande and the highly resistant H7996. We imaged whole roots of plants from each variety obtained at 6 days after inoculation (Fig. S1), a time when plants already showed wilting symptoms (Fig. S2). Marmande roots displayed strong luminescence

intensity, while Shield or H7996 roots displayed low luminescence (Fig. S1A). This phenomenon was consistent regardless of the intensity of signal in the stem or the wilt level and correlated with our previous results using the miniaturized *in vitro* system (Fig. 1).

To quantify the reduced root colonization in resistant varieties, we measured bacterial loads in the taproot at 3 dpi, when susceptible plants start to show symptoms. Bacterial concentrations were calculated from luminescence units measured from taproots with a luminometer, based on the extremely high correlation (r^2 = 0.96, $p<0.0001$) existing between luminescence emitted by the tissue samples and bacterial colony forming units (CFU) (Fig. S3). This experiment revealed that the resistant rootstocks had a significantly reduced mean bacterial density at the root level compared to the susceptible variety, which exhibited bacterial concentrations two orders of magnitude higher (Fig. S1B).

The second bottleneck: Resistant shoots restrict bacterial movement vertically along the xylem

Next, we investigated *R. solanacearum* shoot colonization in soil-inoculated fully developed Marmande, Shield and H7996 plants. Intact, full 4-to-5-week-old plants grown in pots could not be imaged for luminescence due to size limitations and reduced sensitivity due to stem thickness. Thus, we obtained 1-2 cm stem sections up to the third internode from plants 6 days post-inoculation, when wilting symptoms can be observed (Fig. S2). In order to track luminescent bacteria throughout the stem, top and bottom slices of each section were obtained and the remaining stem was longitudinally divided in two. Representative pictures of all sections from a plant of each variety are presented in Figure 3. In all cases, luminescence matched the location of xylem bundles, indicating that bacteria are mostly confined in this tissue at this stage. As expected, bacterial colonization in the shoot was much more apparent in Marmande -as indicated by the intense luminescence observed- compared to the resistant varieties, in which luminescence was in most cases only detected at higher exposure (Fig. 3A and Fig. S4). In addition, the number of luminescent bundles decreased occasionally with height in the resistant varieties, while it remained constant in the susceptible Marmande

plants. In summary, resistant tomato lines display the following stem features after infection: lower number of colonized xylem fiber bundles and some limited bacterial vertical movement along the vessels (Fig. 3).

To avoid plant-to-plant variation in colonization and directly compare the behavior of susceptible and resistant tissues when confronted to equivalent bacterial loads, we characterized *R. solanacearum* distribution in reciprocally grafted plants. We used adult plants inoculated by soil drenching and monitored the vertical movement of the luminescent bacterial strain in the hypocotyl region (where grafting was performed) 6 days after inoculation (Fig. 3B). The number of colonized vessels and luminescence intensity was almost undetectable in the self-grafted resistant H7996 (Fig. 3B top right panel), as had been observed in non-grafted plants (Fig. 3A). Self-grafting of the Marmande variety demonstrated that grafting *per se* did not restrict vertical movement (Fig. 3B top left panel). Interestingly, colonization was hampered in H7996 scions grafted onto Marmande rootstocks and was higher in Marmande scions compared to their grafted H7996 rootstocks (Fig. 3B bottom panels). This demonstrated that at comparable bacterial concentrations, vertical colonization is inhibited and overall bacterial density is strongly reduced along the xylem of H7996 compared to the susceptible Marmande. Similar results were observed in Marmande-Shield grafting combinations (Fig. S5).

A decrease in vertical colonization could be explained by a timing artefact: if luminescence photographs were taken too soon for the bacteria to grow on the resistant scion, that would give a false impression of hampered invasion. To rule out this possibility, we exchanged a fragment of hypocotyl between Marmande and H7996 plants in a double-grafting approach (Fig. S6). Grafted plants contained a 2 cm fragment of the hypocotyl from one of the varieties in-between the basal and distal hypocotyl regions of the other variety (Fig. S6A,B). The double-grafted plants were grown on soil to 7-9 true leaf stage and infected with the luminescent *R. solanacearum* strain (Fig. S6C-G). As expected, plants that contained the roots and basal hypocotyl from Marmande wilted similarly to plants with Marmande rootstocks (Fig. S2, S6D,E). We observed and quantified bacterial movement along the xylem in the two combinations of grafted plants using luminescence (Fig. 4). Marmande rootstocks were

heavily colonized by *R. solanacearum*, and bacterial density decreased as soon as the pathogen crossed the first grafting junction and encountered H7996 tissue. When *R. solanacearum* moved upwards into susceptible tissue for the second time, it multiplied again to high levels (Fig 4A,B top panel and graph). The complementary result was observed in the reciprocal grafting: colonization was hampered in H7996 rootstocks, especially at 10 dpi (Fig S6F,G), reached its peak on Marmande hypocotyls and decreased when *R. solanacearum* crossed the second grafting junction and faced again H7996 tissue (Fig 4A,B bottom panel and graph). Altogether these results demonstrate the ability of H7996 to restrict *R. solanacearum* vertical movement along the xylem in a root-independent manner.

Plant wilting is determined by a bacterial density threshold in the hypocotyl

To trace bacterial vertical movement inside the plant in a quantitative manner, we measured bacterial loads from the taproot to the 3rd internode in >30 plants per grafting combination sampled at different times (3 to 10 dpi), which showed a range of wilting symptoms. The results in Figure 5 clearly show that regardless of the level of susceptibility, asymptomatic tomato plants contain bacterial concentrations generally lower than 10^7 bacterial cells per gram of tissue and wilted plants always show bacterial counts above this threshold in the taproot and basal hypocotyl, although they may hold lower numbers in the shoot above the cotyledons. Additionally, the hypocotyl seems to act as an additional vertical threshold in susceptible plants, since asymptomatic Marmande plants are often colonized below the hypocotyl but the plants always wilt when the bacterium trespasses this level (Fig. 5, top graph). On the contrary, when H7996 scions are grafted on Marmande rootstocks, a situation in which the root barrier of the resistant variety is overcome, the tissues of the resistant variety can cope with high bacterial concentrations in the shoot, thus remaining asymptomatic (Fig. 5, bottom graph). Similar results were observed using the Shield line (Fig. S7).

The third and fourth bottlenecks: Resistant shoots restrict circular and radial bacterial movement

In order to examine the colonization patterns within the stems at the tissue level, we inoculated 4-week old Marmande, H7996 and Shield plants grown in pots with a *R. solanacearum* strain constitutively expressing GFPuv (Cruz *et al*. 2014) and observed shoot slices in a fluorescence stereomicroscope. Figure 6A contains representative images of transversal hypocotyl sections of the three tomato varieties 8 days after inoculation. At this stage, the stem xylem tissue was arranged into four primary bundles, and typically two to four smaller secondary bundles, connected by the inter-fascicular cambium formed by xylem parenchyma and some xylary fibers. The microscopic images indicate that *R. solanacearum* can move from vessel to vessel (circular movement) and from the vessels to the adjacent parenchymatic tissues (radial movement). In the susceptible Marmande, fluorescent bacteria occupy almost entirely the vascular ring and even extend radially to the apoplast of the pith and cortical tissues (Fig. 6A left panels). In contrast, resistant H7996 only exhibited bacteria confined to a few single xylem vessels (Fig. 6A right panels). The moderately resistant variety (Shield) showed an intermediate phenotype with colonization more restricted to the vascular ring and limited radial spread to neighboring tissues (Fig. 6A).

The extremely limited vertical colonization of the xylem in H7996 hampered a precise characterization of the circular and radial bacterial movements in the resistant shoots. To overcome this limitation, we grafted H7996 scions on Marmande rootstocks -a situation that enables high bacterial numbers to reach the resistant stem tissues (Fig. 3B, 4 and 5)- and inoculated these plants using soil drenching with the fluorescent *R. solanacearum* strain. Observation of shoot sections obtained at different shoot heights 8 days post-inoculation indicated extensive vertical, circular and radial colonization of the Marmande tissues below the graft (Fig. 6B and Fig. S8 left panel). In contrast, the section at the graft junction level showed that H7996 tissues immediately blocked the spread of the bacterium circularly through the xylem ring and radially to the pith and cortical tissues (Fig. 6B). These restrictions became more apparent at higher sections, consisting exclusively of resistant tissue (Fig. 6B and Fig. S8 right panel). To better compare the behavior of *R. solanacearum* in resistant and susceptible tissues, we repeated this last experiment using a larger number of plants, and observed under the fluorescence stereomicroscope shoot sections of resistant scions that showed strongest

wilting. Figure 6C shows these H7996 shoot sections confronted with a high bacterial inoculum introduced from the susceptible rootstock, compared to Marmande shoot sections. Noticeably, radial bacterial movement from the highly colonized xylem bundles became strongly restricted in H7996 shoots, even in these extreme cases where the xylem tissue was highly colonized (Fig. 6C right panel). This restriction could also be observed when the fluorescent *R. solanacearum* strain was directly pin-inoculated into the shoots (Fig. S9).

Finally, we performed a time-course invasion assay in which we quantified the amounts of bacteria that were moving outside the vascular ring over time (Fig. 7). We observed that *R. solanacearum* was escaping from the vascular ring as early as 5 dpi and heavily colonized the pith and cortical tissues by 9 dpi (Fig. 7A top panels and 7B). Moreover, the amount of bacteria located outside the vascular tissues was directly correlated with the extent of vascular ring colonization (Fig. 7B). This contrasted with the ability of H7996 shoots to impede pathogen escape from the vascular ring (Fig. 7A top panels, Fig. 7B and Fig. 6). These results indicated that the capacity of *R. solanacearum* to radially invade the pith and cortex tissues is dependent on the level of susceptibility and occurs as a consequence of increased colonization.

DISCUSSION

In this work we propose a model that relates the spatio-temporal dynamics of *R. solanacearum* invasion and proliferation in tomato plants with disease development that shows how quantitative resistance impacts these parameters (Fig. 8). Systematic analysis of bacterial progression inside the plant reveals four clear growth restriction levels in resistant tomato tissues that hamper disease progression: Root colonization, stem vascular bundle invasion, vertical invasion up the vessels, and pith/cortex invasion. The basically binary outcome of death-by-permanent-wilting caused by *R. solanacearum* in tomato seems to require the bacterium to surmount each of these physio-anatomical plant barriers, which is quantitatively defended by host resistance. We discuss below each of these four important levels that can turn the scales towards host resistance or successful plant colonization.

Restriction of root colonization

We analyzed the *R. solanacearum* interaction with tomato using two main variables: susceptible *vs* resistant varieties and soil drenching *vs* pin inoculation. Soil drenching inoculations clearly reproduced the disease progression and the resistance observed in controlled environment studies of comparable conditions and plant age for the different varieties assayed (Fig. S2, Nakaho *et al*. 2004; Wang *et al.*, 1998; McGarvey, Denny and Schell, 1999; Rivard and Louws, 2008). Root pin-inoculation of plantlets grown *in vitro* showed similar results (Fig. 1A), but bacterial concentrations reached higher numbers in the tissues of pin-inoculated compared to soil-drench inoculated resistant varieties, while the susceptible variety was highly colonized in both cases (Figs. 1 & 2 *vs* Fig. S1). These differences in the inoculation method imply that resistant varieties have the ability to restrict root invasion, a step that is overcome when root pin-inoculation is used. Our findings are in agreement with the limited bacterial growth in the taproot of H7996 observed when roots were not wounded prior to inoculation (McGarvey *et al.*, 1999). Additionally, *in vitro* grafted pin-inoculated plants display slightly delayed colonization than non-grafted plants (3 dpi on Fig. 1A *vs* 5 dpi on Fig. 2). This might be linked to its developmental stage. Since older plants (in this case the grafted ones) are more developed, their cell walls might be reinforced, thus partly hindering *R. solanacearum* invasion. Finally, the pin-inoculated resistant plants that are highly colonized likely mimic the situation encountered in nature when environmental conditions are highly favorable to the pathogen. Indeed, it has been shown that even the most highly resistant varieties available do not completely prevent root and stem colonization by *R. solanacearum* in greenhouse conditions (Nakaho 1997a; Nakaho 1997b; Nakaho et al. 2004).

Restriction of vertical movement up the stem

The fact that *R. solanacearum* can colonize the stems of many resistant tomato plants when soil-drench inoculation is used, indicates that additional resistance mechanisms must be also in place at the aerial tissue level to prevent wilting. Previous studies had demonstrated that bacterial counts in stems of resistant tomato plants were always

lower than in susceptible varieties and that this was due to a limitation of pathogen movement from the primary xylem to other xylem tissues (Nakaho *et al.*, 2004). In this work, we have analyzed the vertical dimension of the bacterial spread and demonstrated that resistant tissues limit movement upwards in the xylem vessels (Fig. 3). Double grafting experiments, where a small portion of resistant stem is introduced in an otherwise susceptible adult plant or vice-versa, rule out any effect of grafting *per se* in bacterial movement inside the xylem and suggest that resistance to bacterial wilt could be due to non-diffusible xylematic structures/compounds originating from the stem, as has been described for other bacterial vascular diseases (Chatterjee *et al.*, 2008).

The nature of the plant components or structures hindering root-to-shoot vertical bacterial movement is still unknown, although classical reports described the presence of tyloses -evaginations of the adjacent parenchyma cells into the xylem lumen- and gums that seemed to limit bacterial spread in the xylem of bacterial wilt-resistant Caraïbo tomato plants (Grimault *et al.*, 1994*b*). Obstruction of xylem vessels by gums and tyloses is a common plant response designed to restrict the systemic infection of vascular pathogens (VanderMolen, *et al.*, 1987; Grimault *et al.*, 1994; Clérivet *et al.*, 2000; Sun *et al.*, 2013). For instance, vascular gelation is considered an essential part of the Fusarium wilt resistance in carnation plants (Baayen and Elgersma, 1985). Tyloses have been similarly proposed to restrict pathogen movement in tomato cultivars resistant to the vascular pathogens *Fusarium oxysporum, Verticillium abo-atrum,* and *R. solanacearum* (Hutson and Smith, 1980; VanderMolen *et al.*, 1987; Grimault *et al.*, 1994*b*). Although Grimault et al. correlated tylose presence in Caraïbo to limitation of *R. solanacearum* spread, in another resistant cultivar (LS-89) the formation of these structures was neither induced by the pathogen nor seemed to affect bacterial colonization (Nakaho, 1997*a*). Similarly, tyloses formed in grapevines in response to *Xylella fastidiosa* infection were found more abundant in susceptible cultivars and did not affect the pathogen's vertical movement (Sun *et al.*, 2013). This suggests that the role of tyloses in vascular pathogen restriction may be cultivar- or species-specific and/or depend on the lignification status of the plant host. The results presented here and our recent finding that *R. solanacearum* tolerant potato lines also induced the

development of tyloses upon infection (Ferreira *et al.*, 2017) seem to indicate that these structures are important players for bacterial wilt resistance in solanaceous plants.

Restriction of vascular bundle invasion and the bacterial density threshold

Restriction of *R. solanacearum* colonization in stems of H7996 is also achieved by limiting its horizontal movement vessel-to-vessel (referred hereafter as circular movement). Confinement of *R. solanacearum* to primary xylem vessels has been observed in stems and roots of different resistant tomato cultivars compared to susceptible ones (Nakaho, 1997*a*; Nakaho *et al.*, 2004; Caldwell *et al.*, 2017). A similar correlation between *R. solanacearum* movement between stem vessels, bacterial growth and the level of susceptibility has been observed in potato (Cruz *et al.*, 2014; Ferreira *et al.*, 2017). Similarly, *X. fastidiosa* has been shown to invade ten times fewer stem vessels and exhibit lower population densities in resistant cultivars (Chatterjee *et al.*, 2008). These results indicate that limitation of circular movement in the xylem ring is a conserved mechanism for resistance against vascular bacterial pathogens. Restriction of *R. solanacearum* into the primary xylem could explain why resistant tomato plants often remain asymptomatic. If a blockage occurs in the primary xylem, which is largely non-functional after the secondary xylem is produced (Esau, 1977), the infection-free secondary xylem could perform flow conduction undisturbed.

R. solanacearum can move horizontally through the xylem ring by directly degrading cell walls of primary xylem vessels or pit membranes in secondary xylem vessels of susceptible plants (Wallis and Truter, 1978; Grimault *et al.*, 1994*b*; Vasse *et al.*, 1995; Nakaho *et al.*, 2000). To counter such circular movement, plants have evolved structural defenses induced upon attack by vascular pathogens that involve the deposition of various coating materials to reinforce the walls of xylem vessels, pit membranes and surrounding parenchyma cells. Vascular coatings are thicker in resistant tomato cultivars infected with *R. solanacearum* and may be the cause for the observed limitation of bacterial movement between xylem tissues (Nakaho *et al.*, 2000, 2004). The detailed description of the process we present here will be crucial to decipher the genetic determinants and the composition of these vascular coatings, which remain unknown.

Circular restriction in the stem is a very efficient confinement strategy, since it is still acting when high loads of bacteria are forced into the stem through root-inoculations using H7996 scions grafted onto Marmande rootstocks (Fig. 6). However, there seems to be an upper limit of bacterial inoculum beyond which this restriction is no longer effective (see Plant number 4 in Fig. 6C lower panel). This is in agreement with previous reports showing that delivering a high *R. solanacearum* inoculum (10^9 CFU ml^{-1}) directly in tomato stems overcomes resistance (Nakaho, 1997*b*). This idea relates to the concept of a density threshold in the interaction between tomato and *R. solanacearum*. Earlier observations established the onset of bacterial wilt symptoms at a density in the stem between 10^6 and 10^8 CFU g^{-1} of fresh tissue (Grimault and Prior, 1994; Nakaho, 1997*a*; Huang and Allen, 2000; Nakaho *et al.*, 2004). We have characterized this threshold systematically assessing bacterial densities throughout the plant in large populations of grafted tomatoes with varying resistance. We conclude that, both in resistant and in susceptible varieties, symptom appearance invariably takes place when bacterial populations in the hypocotyl exceed a threshold of 10^7 CFU per gram of tissue (Fig. 5 and Fig. S7). Plating dilutions of homogenized tissues is labor intensive, but we show that light emission from tissues inoculated with a luminescent strain is a useful measure of bacterial counts (correlation coefficient 0.9). Since bacterial density and distribution is predictive of the degree of disease resistance, we have started using luminescent strains to screen potato germplasm for resistance to bacterial wilt as a way to aid the breeding process (Cruz *et al.*, 2014; Ferreira *et al.*, 2017).

Restriction of the radial movement "out of the xylem" into the pith and cortex

Finally, our characterization has revealed an additional level limiting bacterial spread in the tissues of resistant tomato varieties: restriction of *R. solanacearum* radial movement out of the xylem into the adjacent parenchyma cells in the pith and cortex (Figs. 6 & 7). These metabolically active cells are in close contact with the xylem vessels through the pits and are thought to be pivotal for the induction of plant defense against xylematic pathogens, although very little is known about the mechanisms regulating this response. Earlier works detected widespread *R. solanacearum* colonization of stem parenchyma cells in susceptible tomato varieties at late stages of infection, when plants showed

558 extensive wilting (Nakaho, 1997*a*; Nakaho *et al.*, 2000). These cells appeared filled with
559 bacteria and displayed necrosis symptoms and signs of degeneration. On the contrary,
560 in resistant tomato varieties, necrotic parenchyma cells containing bacteria were
561 observed occasionally (Nakaho *et al.*, 2000). Our data confirm these observations and
562 additionally show that parenchyma cell invasion starts at earlier times (5 dpi) in
563 susceptible plants and spreads massively through the pith at late time points (8-9 dpi,
564 Fig. 7A). In contrast, colonization remains limited to xylem vessels in resistant tomato
565 (Fig. 6).
566 As for the previously described bacterial movements, radial restriction out of the xylem
567 in resistant varieties can be partially overridden by grafting to susceptible rootstocks that
568 enable high bacterial densities to access resistant tissues, as can be seen in some of
569 the images in Fig. 6C. This is in agreement with a previous report showing that when
570 high bacterial inocula were used (10^9), *R. solanacearum* could also be detected in the
571 parenchyma cells of resistant tomato (Nakaho, 1997*b*). Thus, restriction of radial
572 bacterial movement is no longer effective when bacterial densities surpass a certain
573 threshold.
574 Structural changes in cell walls and pit membranes in response to *R. solanacearum*
575 infection are more conspicuous in resistant tomato (Nakaho et al., 2000). Thus, bacteria
576 may be prevented to escape the xylem in resistant tomato by a combination of inducible
577 structural defense mechanisms that may appear later and/or with less intensity in
578 susceptible lines, rendering them ineffective to restrict colonization. Very interestingly,
579 slightly decreased invasion can also be observed in the susceptible hypocotyls of the
580 Marmande-H7996 grafting combination (Fig. 7). This finding could be explained by a
581 cross-talk between scion and rootstock. Such interaction could trigger the expression of
582 putative defense-related genes or genes that reinforce plant cell-wall structures on the
583 susceptible rootstock. Alternatively, defense-related or structure-remodeler proteins
584 might be secreted by the resistant scion and reinforce nearby tissues (in this case the
585 susceptible hypocotyl). The two explanations seem plausible given the existing vascular
586 connectivity between the grafted counter parts. Indeed, a transcriptional reprogramming
587 occurs even in rootstocks and scions of the tomato/potato heterografting system (Zhang
588 *et al.*, 2019). Additionally, peroxidases and other cell wall remodeling enzymes –such as

glycosyl hydrolases– are secreted into the xylem by the resistant H7996 upon *R. solanacearum* infection (Planas-Marquès *et. al.* unpublished). Hence, an increased lignification and cell wall reinforcement status could also take place in neighboring susceptible tissues in grafted plants.

An integrated model for tomato resistance to bacterial wilt

As we have discussed, in the last three decades, various labs have aimed at understanding how resistant tomato varieties restrict *Ralstonia solanacearum* colonization and remain asymptomatic despite holding relatively high bacterial loads. The fact that the battlefield is not limited to a particular plant site -the bacterium has to traverse different tissues in order to reach the xylem- has complicated this work. But, is the xylem the final goal of *R. solanacearum*?

Here, we have defined the barriers encountered by *R. solanacearum* as it progresses from the soil into the xylem and have found that after systematic spread through the xylem the final destination of the bacterium may be extensive invasion of the stem apoplast. It has already been suggested that vascular bacteria use plant cell-wall degradation products as carbon and energy sources (Chatterjee *et al.*, 2008; Genin and Denny, 2012). It is then tempting to speculate that *R. solanacearum* has evolved not only to colonize the xylem but to escape from it to obtain richer nutrition sources from metabolically active parenchyma cells, facilitating the decay of infected plants to spread in the soil and move into the next host.

In conclusion, we clearly define four bottlenecks to bacterial colonization in tomato and demonstrate that the degree of resistance of a given variety correlates with its capacity to restrict bacterial movement at these levels. Restriction at all levels makes H7996 the most resistant tomato line, consistent with the polygenic nature of its resistance (Wang *et al.*, 2013) that has made introgression breeding extremely difficult (Scott *et al.*, 2005; Hanson *et al.*, 2016). We conceive this integrative study as a first step towards the characterization of the genetic and molecular determinants that govern resistance on each stage of *R. solanacearum* invasion.

SUPPLEMENTARY DATA

Fig. S1. Measurement of bacterial root colonization in tomato plants.

Fig. S2. Symptom development over time in grafted tomato plants.

Fig. S3. Correlation between luminescence and bacterial counts.

Fig. S4. *R. solanacearum* vertical movement in tomato shoots as seen by different intensities of exposure.

Fig. S5. *R. solanacearum* vertical movement in the shoots of Marmande and Shield grafted plants.

Fig. S6. Double-grafted plants disease evolution over time.

Fig. S7. *R. solanacearum* bacterial density assessed over the height of grafted tomato plants.

Fig. S8. Circular and radial invasion of *R. solanacearum* in susceptible and resistant tomato shoots.

Fig. S9. Invasion of *R. solanacearum* in susceptible and resistant pin-inoculated tomato shoots.

AKNOWLEDGEMENTS

This work was funded by projects AGL2016-78002-R to N.S.C. and M.V., and RyC 2014-16158 to N.S.C. (Spanish Ministry of Economy and Competitiveness). JPK was supported partially by the USDA NIFA Grants # 2011-51181-30963 and 2016-51181-25404 to FJL and DRP, and a Monsanto Graduate Fellowship award through North Carolina State University. We acknowledge financial support from the “Severo Ochoa Program for Centers of Excellence in R&D” (SEV-2015-0533) and the CERCA Program from the Catalan Government (Generalitat de Catalunya).

AUTHOR CONTRIBUTION

M. P-M. Designed the research, performed the research; analyzed and interpreted data and wrote the manuscript

650 J. P. K. Performed the research; analyzed and interpreted data and wrote the
651 manuscript
652 A .K. Performed the research and analyzed data
653 D.R.P. Designed the research and interpreted data
654 F.J.L. Designed the research and interpreted data
655 N.S C. Designed the research, analyzed and interpreted data and wrote the manuscript
656 M.V. Designed the research, analyzed and interpreted data and wrote the manuscript

REFERENCES

657 **Baayen RP, Elgersma DM**. 1985. Colonization and histopathology of susceptible and
658 resistant carnation cultivars infected with Fusarium oxysporum f. sp. dianthi.
659 Netherlands Journal of Plant Pathology **91**, 119–135.
660 **Caldwell D, Kim B, Iyer-pascuzzi AS**. 2017. Ralstonia solanacearum differentially
661 colonizes roots of resistant and susceptible tomato plants Denise. Phytopathology **107**,
662 528–536.
663 **Carmeille A, Caranta C, Dintinger J, Prior P, Luisetti J, Besse P**. 2006. Identification
664 of QTLs for Ralstonia solanacearum race 3-phylotype II resistance in tomato.
665 Theoretical and Applied Genetics **113**, 110–121.
666 **Chatterjee S, Newman KL, Lindow SE**. 2008. Cell-to-Cell Signaling in Xylella
667 fastidiosa Suppresses Movement and Xylem Vessel Colonization in Grape . Molecular
668 Plant-Microbe Interactions **21**, 1309–1315.
669 **Clérivet A, Déon V, Alami I, Lopez F, Geiger J-P, Nicole M**. 2000. Tyloses and gels
670 associated with cellulose accumulation in vessels are responses of plane tree seedlings
671 (Platanus × acerifolia) to the vascular fungus Ceratocystis fimbriata f. sp platani. Trees
672 **15**, 25–31.
673 **Cruz APZ, Ferreira V, Pianzzola MJ, Siri MI, Coll NS, Valls M**. 2014. A novel,
674 sensitive method to evaluate potato germplasm for bacterial wilt resistance using a
675 luminescent Ralstonia solanacearum reporter strain. Molecular plant-microbe
676 interactions : MPMI **27**, 277–285.

Esau K. 1977. *Anatomy of Seed Plants*. New York: Wiley.

Ferreira V, Pianzzola MJ, Vilaró FL, Galván GA, Tondo ML, Rodriguez M V, Orellano EG, Valls M, Siri MI. 2017. Interspecific Potato Breeding Lines Display Differential Colonization Patterns and Induced Defense Responses after Ralstonia solanacearum Infection. Frontiers in Plant Science **8**, 1–14.

Genin S. 2010. Molecular traits controlling host range and adaptation to plants in Ralstonia solanacearum. New Phytologist **187**, 920–928.

Genin S, Denny TP. 2012. Pathogenomics of the Ralstonia solanacearum Species Complex. Annual Review of Phytopathology **50**, 67–89.

Grimault V, Anais G, Prior P. 1994*a*. Distribution of Pseudomonas solanacearum in the stem tissues of tomato plants with different levels of resistance to bacterial wilt. Plant Pathotogy **43**, 663–668.

Grimault V, Gélie B, Lemattre M, Prior P, Schmit J. 1994*b*. Comparative histology of resistant and susceptible tomato cultivars infected by Pseudomonas solanacearum. Physiological and Molecular Plant Pathology **44**, 105–123.

Grimault V, Prior P. 1993. Bacterial wilt resistance in tomato associated with tolerance of vascular tissues to Pseudomonas solanacearum. Plant Pathology **42**, 589–594.

Grimault V, Prior P. 1994. Grafting Tomato Cultivars Resistant or Susceptible to Bacterial Wilt - Analysis of Resistance Mechanisms. Journal of Phytopathology **141**, 330–334.

Hanson P, Lu SF, Wang JF, *et al.* 2016. Conventional and molecular marker-assisted selection and pyramiding of genes for multiple disease resistance in tomato. Scientia Horticulturae **201**, 346–354.

Hayward AC. 1991. Biology and Epidemiology of Bacterial Wilt Caused by Pseudomonas Solanacearum. Annual Review of Phytopathology **29**, 65–87.

Hayward AC. 1994. The Hosts of Pseudomonas solanacearum. In: Hayward AC,, In: Hartman GL, eds. Bacterial Wilt: The Disease and Its Causative Agent, Pseudomonas solanacearum. Wallingford, UK: CAB International, 9–24.

Huang Q, Allen C. 2000. Polygalacturonases are required for rapid colonization and full virulence of Ralstonia solanacearum on tomato plants. Physiological and Molecular Plant Pathology **57**, 77–83.

Hutson RA, Smith IM. 1980. Phytoalexins and tyloses in tomato cultivars infected with Fusarium oxysporum f.sp. lycopersici or Verticillium albo-atrum. Physiological Plant Pathology **17**, 245–257.

Ishihara T, Mitsuhara I, Takahashi H, Nakaho K. 2012. Transcriptome Analysis of Quantitative Resistance-Specific Response upon Ralstonia solanacearum Infection in Tomato. PLoS ONE **7**.

Kim BS, French E, Caldwell D, Harrington EJ, Iyer-Pascuzzi AS. 2015. Bacterial wilt disease: Host resistance and pathogen virulence mechanisms. Physiological and Molecular Plant Pathology **95**, 37–43.

Kunwar S, Iriarte F, Fan Q, *et al.* 2018. Transgenic Expression of EFR and Bs2 Genes for Field Management of Bacterial Wilt and Bacterial Spot of Tomato. Phytopathology **108**, 1402–1411.

Mangin B, Thoquet P, Olivier J, Grimsley NH. 1999. Temporal and multiple quantitative trait loci analyses of resistance to bacterial wilt in tomato permit the resolution of linked loci. Genetics **151**, 1165–1172.

Mansfield J, Genin S, Magori S, *et al.* 2012. Top 10 plant pathogenic bacteria in molecular plant pathology. Molecular Plant Pathology **13**, 614–629.

McGarvey J a, Denny TP, Schell M a. 1999. Spatial-Temporal and Quantitative Analysis of Growth and EPS I Production by Ralstonia solanacearum in Resistant and Susceptible Tomato Cultivars. Phytopathology **89**, 1233–1239.

Nakaho K. 1997*a*. Distribution and Multiplication of Ralstonia solanacearum (Synonym Pseudomonas solanacearum) in Tomato Plants of Resistant Rootstock Cultivar LS-89 and Susceptible Ponderosa. Ann Phytopathol Soc Jpn **63**, 83–88.

Nakaho K. 1997*b*. Distribution and multiplication of *Ralstonia solanacearum*in stem-inoculated tomato rootstock cultivar LS-89 resistant to bacterial wilt. Ann. Phytopathol. Soc. Jpn **63**, 341–344.

Nakaho K, Hibino H, Miyagawa H. 2000. Possible mechanisms limiting movement of Ralstonia solanacearum in resistant tomato tissues. Journal of Phytopathology **148**, 181–190.

Nakaho K, Inoue H, Takayama T, Miyagawa H. 2004. Distribution and multiplication of Ralstonia solanacearum in tomato plants with resistance derived from different origins.

739 Journal of General Plant Pathology **70**, 115–119.
740 **Planas-Marquès M, Bernardo-Faura M, Paulus P, Kaschani F, Kaiser M, Valls M,**
741 **van Der Hoorn R, Coll N**. 2018. Protease Activities Triggered by Ralstonia
742 solanacearum Infection in Susceptible and Tolerant Tomato Lines. Mol Cell Proteomics
743 **17**, 1112–1125.
744 **Prior P, Bart S, Leclercq S, Darrasse a, Anais G**. 1996. Resistance to bacterial wilt in
745 tomato as discerned by spread of Pseudomonas (Burholderia) solanacearum in the
746 stem tissues. Plant Pathology **45**, 720–726.
747 **Rivard CL, Louws FJ**. 2008. Grafting to manage soilborne diseases in heirloom tomato
748 production. HortScience **43**, 2104–2111.
749 **Schell MA**. 2000. Control of Virulence and Pathogenicity Genes of Ralstonia
750 Solanacearum by an Elaborate Sensory Network. Annual Review of Phytopathology **38**,
751 263–292.
752 **Scott JW, Wang JF, Hanson PM**. 2005. Breeding Tomatoes for Resistance to
753 Bacterial Wilt, a Global View. Acta Horticulturae **695**, 161–172.
754 **Suchoff D, Gunter C, Schultheis J, Louws FJ**. 2015. On-farm grafted tomato trial to
755 manage bacterial wilt. Acta Horticulturae **1086**, 119–128.
756 **Sun Q, Sun Y, Walker MA, Labavitch JM**. 2013. Vascular Occlusions in Grapevines
757 with Pierce's Disease Make Disease Symptom Development Worse. Plant Physiology
758 **161**, 1529–1541.
759 **Thoquet P, Olivier J, Sperisen C, Rogowsky P, Laterrot H, Grimsley N**. 1996*a*.
760 Quantitative trait loci determining resistance to bacterial wilt in tomato cultivar
761 Hawaii7996. Molecular plant-microbe interactions : MPMI **9**, 826–836.
762 **Thoquet P, Olivier J, Sperisen C, Rogowsky P, Prior P, Anais G, Mangin B, Bazin**
763 **B, Nazer R, Grimsley N**. 1996*b*. Polygenic resistance of tomato plants to bacterial wilt
764 in the French West Indies. Molecular plant-microbe interactions : MPMI **9**, 837–842.
765 **VanderMolen GE, Beckman CH, Rodehorst E**. 1987. The ultrastructure of tylose
766 formation in resistant banana following inoculation with Fusarium oxysporum f.sp.
767 cubense. Physiological and Molecular Plant Pathology **31**, 185–200.
768 **Vasse J, Frey P, Trigalet A**. 1995. Microscopic studies of intercellular infection and
769 protoxylem invasion of tomato roots by Pseudomonas solanacearum. Molecular plant-

770 microbe interactions□: MPMI **8**, 241–251.
771 **Wallis FM, Truter SJ**. 1978. Histopathology of tomato plants infected with
772 Pseudomonas solanacearum, with emphasis on ultrastructure. Physiological Plant
773 Pathology **13**, 307–310.
774 **Wang JF, Hanson P, Barnes J**. 1998. Worldwide evaluation of an international set of
775 resistance sources to bacterial wilt in tomato. In: Prior P,, In: Allen C,, In: Elphinstone J,
776 eds. Bacterial Wilt Disease: Molecular and Ecological Aspects. Berlin: Springer, 269–
777 275.
778 **Wang JF, Ho FI, Truong HTH, Huang SM, Balatero CH, Dittapongpitch V, Hidayati**
779 **N**. 2013. Identification of major QTLs associated with stable resistance of tomato
780 cultivar 'Hawaii 7996' to Ralstonia solanacearum. Euphytica **190**, 241–252.
781 **Wang JF, Olivier J, Thoquet P, Mangin B, Sauviac L, Grimsley NH**. 2000.
782 Resistance of tomato line Hawaii7996 to Ralstonia solanacearum Pss4 in Taiwan is
783 controlled mainly by a major strain-specific locus. Molecular plant-microbe
784 interactions□: MPMI **13**, 6–13.
785 **Zhang G, Mao Z, Wang Q, Song J, Nie X, Wang T, Zhang H, Guo H**. 2019.
786 Comprehensive transcriptome profiling and phenotyping of rootstock and scion in a
787 tomato/potato heterografting system. Physiologia Plantarum **166**, 833–847.

FIGURE LEGENDS

Fig. 1. Non-destructive time course evaluation of *R. solanacearum* colonization in in vitro grown resistant and susceptible tomato plants. Tomato seedlings of the susceptible Marmande or the resistant Hawaii 7996 (H7996) varieties were pin-inoculated at the root level with a luminescent *R. solanacearum* strain and colonization and wilting symptoms were evaluated over time. A) Percentage of plants showing wilting symptoms. B) Percentage of plants colonized in the roots and stems based on luminescence signal emitted by the reporter strain. C) Representative photograph showing infected seedlings at 4 days post-inoculation (dpi). The plant outline is due to background light from photosynthetic tissues, while luminescence is detected as darker areas. Saturation level was never reached. The experiment was repeated three times with similar colonization kinetics. n=20 plants per variety.

Fig. 2. Bacterial shoot colonization in Marmande and Hawaii 7996 grafted plants. Tomato seedlings of Marmande and H7996 were grafted at the level of the mid-stem (A) or root collar (B) and were then pin-inoculated at the root level with the luminescent *R. solanacearum* strain. A representative photograph of reciprocally grafted plants is shown for each grafting type at 10 dpi. The percentage of plants colonized in the roots and tissues immediately below and above the graft are shown next to the photographs. Arrowheads point the grafting junction. Both experiments were repeated at least three times with similar colonization kinetics. In A, n=7-8 plants per grafting combination; in B, n=12-15.

Fig. 3. *R. solanacearum* vertical movement in tomato shoots. Four-to-six week-old tomato plants of non-grafted susceptible Marmande, the moderately resistant Shield variety, and the highly resistant H7996 (A) and reciprocally grafted Marmande and H7996 plants (B) grown in pots were soil inoculated with the luminescent *R. solanacearum*. Shoot sections were obtained at 6 dpi and photographed in a live imager. In (A), photographs represent each bisected fragment and its top and bottom slices exposed. Sections were obtained at the base of the hypocotyl, the distal

hypocotyl (right below the cotyledons), and the internodes 1, 2 and 3. In the Image Lab software (Bio-Rad) the following 'High'/'Low'/'Gamma' values were used for low and high exposure settings, respectively: 10000/60/1 and 1300/60/2. In (B), sections were obtained above and below the graft junction. The arrowheads and dotted lines indicate the position of the graft junction.

Fig. 4. Bacterial shoot colonization in Marmande and H7996 double-grafted plants. Tomato seedlings of Marmande and H7996 were double-grafted at the middle of the stem, transferred on pots and grown for 3-4 weeks. Then they were soil-inoculated with the luminescent *R. solanacearum* strain. A) Shoot sections from the hypocotyl were obtained at 10 (top panel) or 23 (bottom panel) dpi and photographed in a live imager. "Bottom" and "Top" refer to Basal and Distal hypocotyl locations, whereas "Middle" refers to the region in between the two graft junctions (arrowheads and dotted lines). B) Bacterial loads were quantified in the shoots of the plants shown on (A) using the luminescence-CFU correlation.

Fig. 5. *R. solanacearum* bacterial density assessed over the height of grafted asymptomatic tomato plants. Bacterial concentrations at different heights in the tissues of wilting (light grey) and asymptomatic (dark grey) grafted plants. Luminescence was measured with a luminometre in 0.5 cm sections from at least 30 inoculated plants per grafting combination. Bacterial counts were calculated from luminescence and are expressed as log CFU g^{-1} tissue. Each dot represents one plant. Only one self-grafted H7996 plant wilted, hence the lack of boxplot. Values between 0 and 4 lie below the threshold for luminescence detection (see Supplementary Figure S3) and are here considered as zeros. From left to right, sections correspond to: taproot, basal hypocotyl, distal hypocotyl, internodes 1, 2 and 3. The dashed red line highlights the location of the grafting union. Letters above each boxplot indicate significant statistical difference by Fisher's LSD (α=0.05). Within each boxplot, the whiskers extend from the hinges to the largest (upper whisker) or smallest (lower whisker) value no further than 1.5 * IQR from the hinge (where IQR is the inter-quartile

range, or distance between the first and third quartiles). Dots beyond the end of the whiskers are outliers. The band inside each box indicates the median.

Fig. 6. Distribution of a fluorescent *R. solanacearum* strain in susceptible and resistant tomato shoots. A) Four-to-five week-old tomato plants of the susceptible Marmande, the moderately resistant Shield variety, and the highly resistant H7996 grown in pots were soil-inoculated with a fluorescent *R. solanacearum* strain. Basal hypocotyl stem sections were obtained and photographed in a fluorescence stereomicroscope under white (top panels) and UV light (middle and lower panels). Lower panels show a magnification of the indicated square areas. The sections were visualized through a UV light filter, highlighting the autofluorescence of lignin in blue and the fluorescence emitted by the bacteria in green. Green dots correspond to bacterial clumps. Arrowheads mark xylem vessels with limited colonization. B) Grafted plants containing H7996 scions on Marmande rootstocks were grown and inoculated with the fluorescent strain as described and transversal sections taken at different heights below and above the graft junction were photographed in a fluorescence stereomicroscope. C) Fluorescence photographs of highly colonized and fully wilted Marmande and H7996 shoots at the basal hypocotyl and first internode.

Fig. 7. Time-course invasion of the fluorescent *R. solanacearum* strain in grafted tomato shoots. A) Fluorescence photographs of self-grafted Marmande and plants containing H7996 scions on Marmande rootstocks inoculated with the fluorescent *R. solanacearum* strain. Sections were taken at the basal hypocotyl (bottom photograph) and first internode (top photograph). The sections were visualized through a UV light filter, highlighting the autofluorescence of lignin in blue and the fluorescence emitted by the bacteria in green. B) Quantification of fluorescence signal (AU, Arbitrary Units) in the vascular ring and outside areas in basal hypocotyl (bottom graph) and first internode (top graph) locations in three biological replicates (n=3) of plants from each stage of the infection shown in (A). Error bars indicate standard error. Letters above each bar indicate significant statistical difference by Fisher's LSD (α=0.05).

Fig. 8. Tug-of-war model of the tomato-*R. solanacearum* pathosystem in susceptible and resistant germplasm. Schematic representation of the colonization movements of *R. solanacearum* (green) inside susceptible and resistant tomato tissues.

FIGURES

Fig. 1

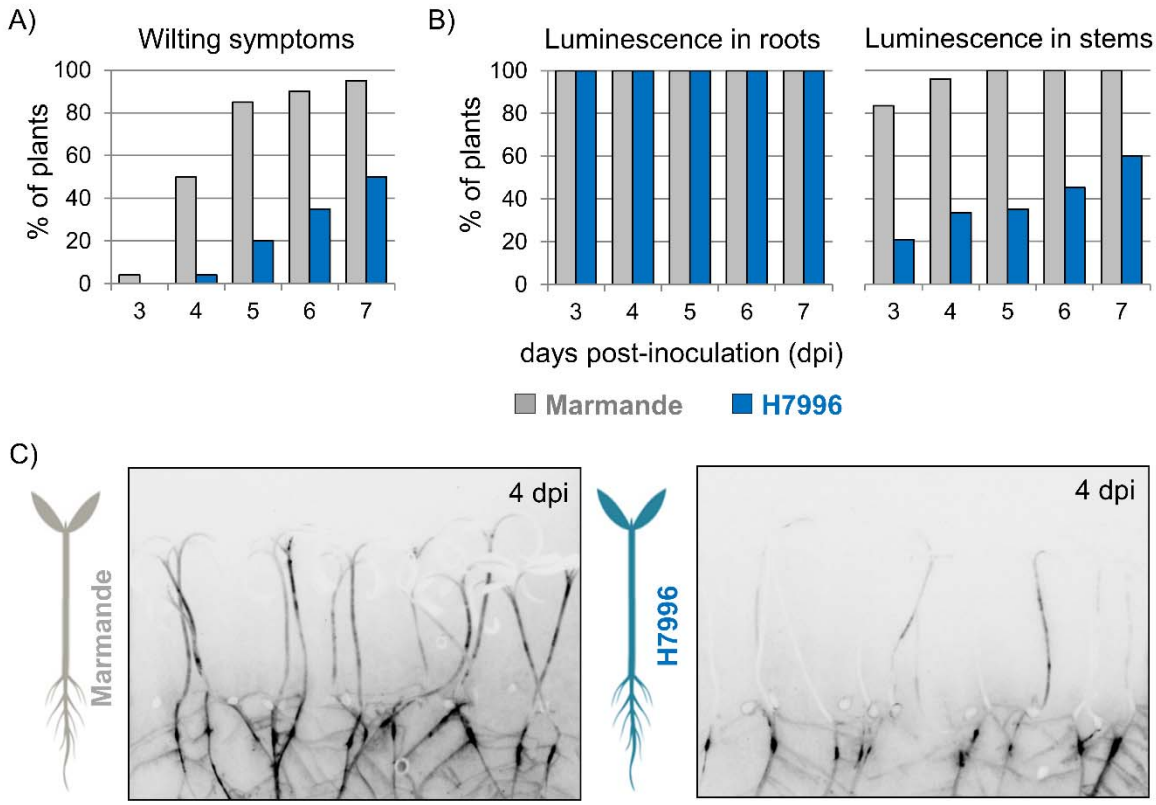

Fig. 2

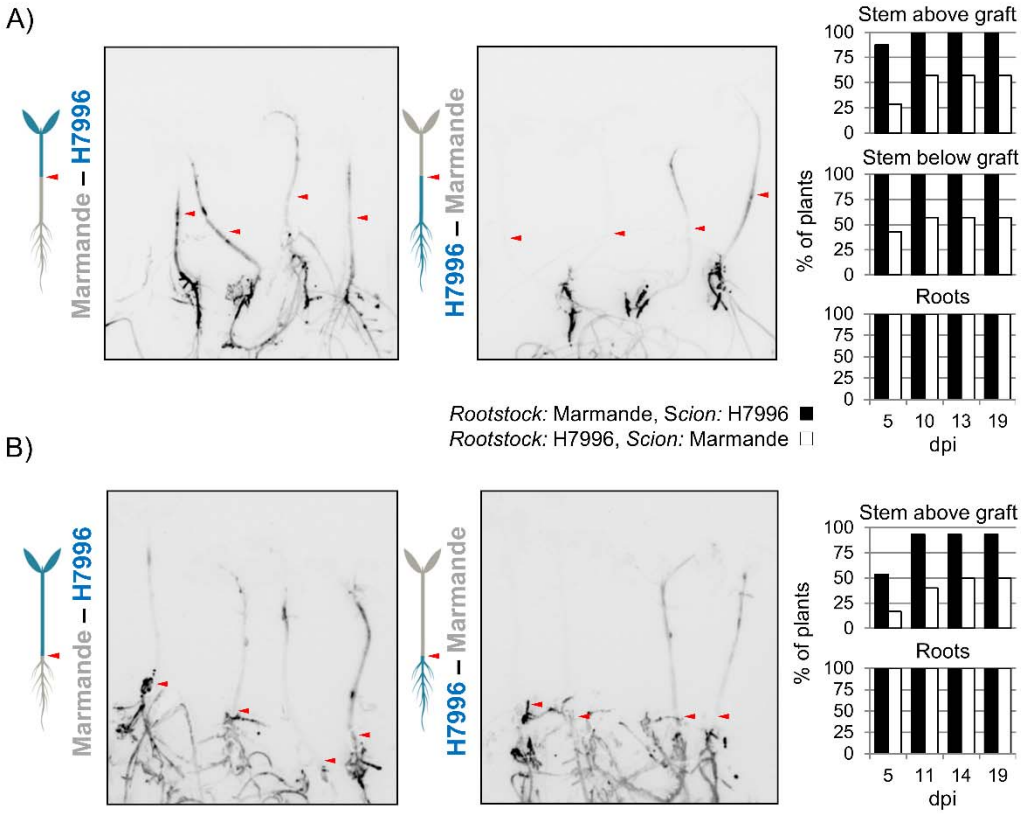
A)
Marmande – H7996
H7996 – Marmande
Stem above graft
Stem below graft
Roots
% of plants
100
75
50
25
0
5 10 13 19
dpi
Rootstock: Marmande, Scion: H7996
Rootstock: H7996, Scion: Marmande
B)
Marmande – H7996
H7996 – Marmande
Stem above graft
Roots
% of plants
100
75
50
25
0
5 11 14 19
dpi

Fig. 3

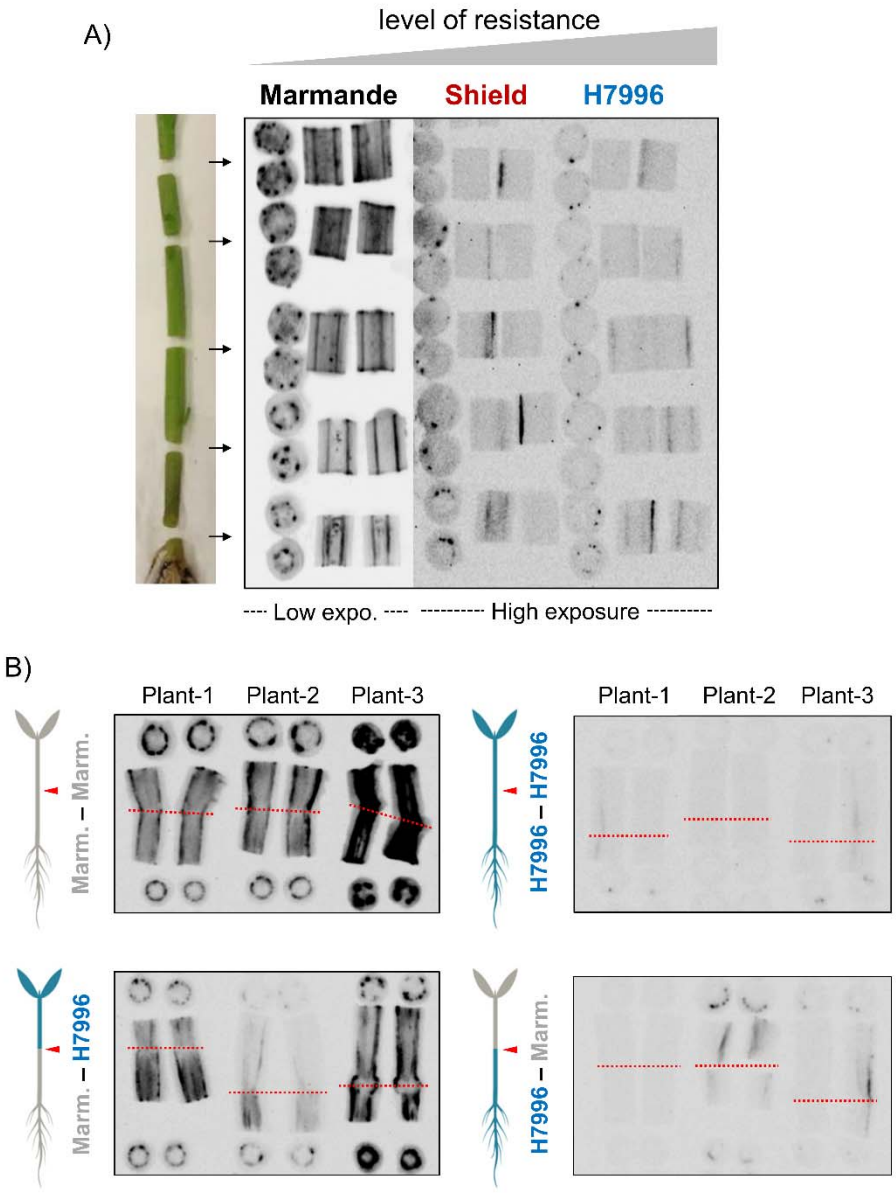
A)
level of resistance
Marmande
Shield
H7996
---- Low expo. ---- ---------- High exposure ----------
B)
Plant-1
Plant-2
Plant-3
Marm. – Marm.
H7996 – H7996
Marm. – H7996
H7996 – Marm.

Fig. 4

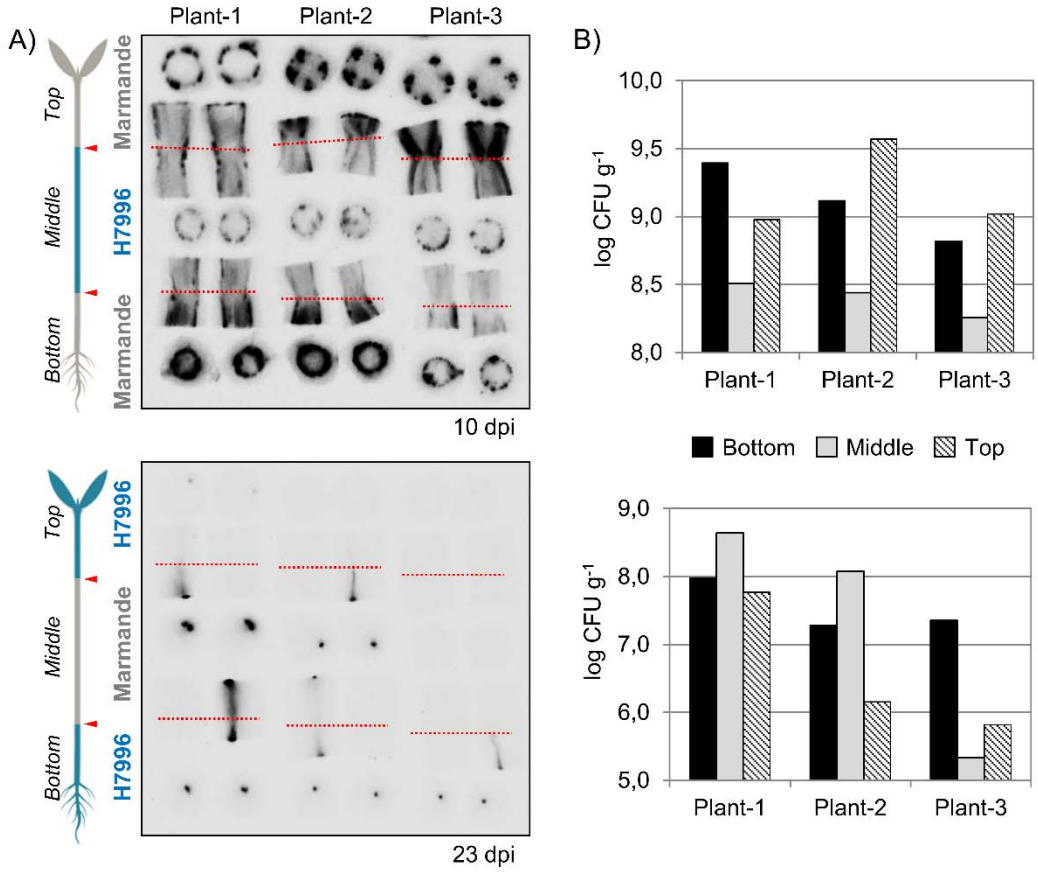
A)
Plant-1
Plant-2
Plant-3
Top
Middle
Bottom
Marmande
H7996
Marmande
10 dpi
Top
Middle
Bottom
H7996
Marmande
H7996
23 dpi
B)
log CFU g-1
10,0
9,5
9,0
8,5
8,0
Plant-1
Plant-2
Plant-3
Bottom
Middle
Top
log CFU g-1
9,0
8,0
7,0
6,0
5,0
Plant-1
Plant-2
Plant-3

Fig. 5

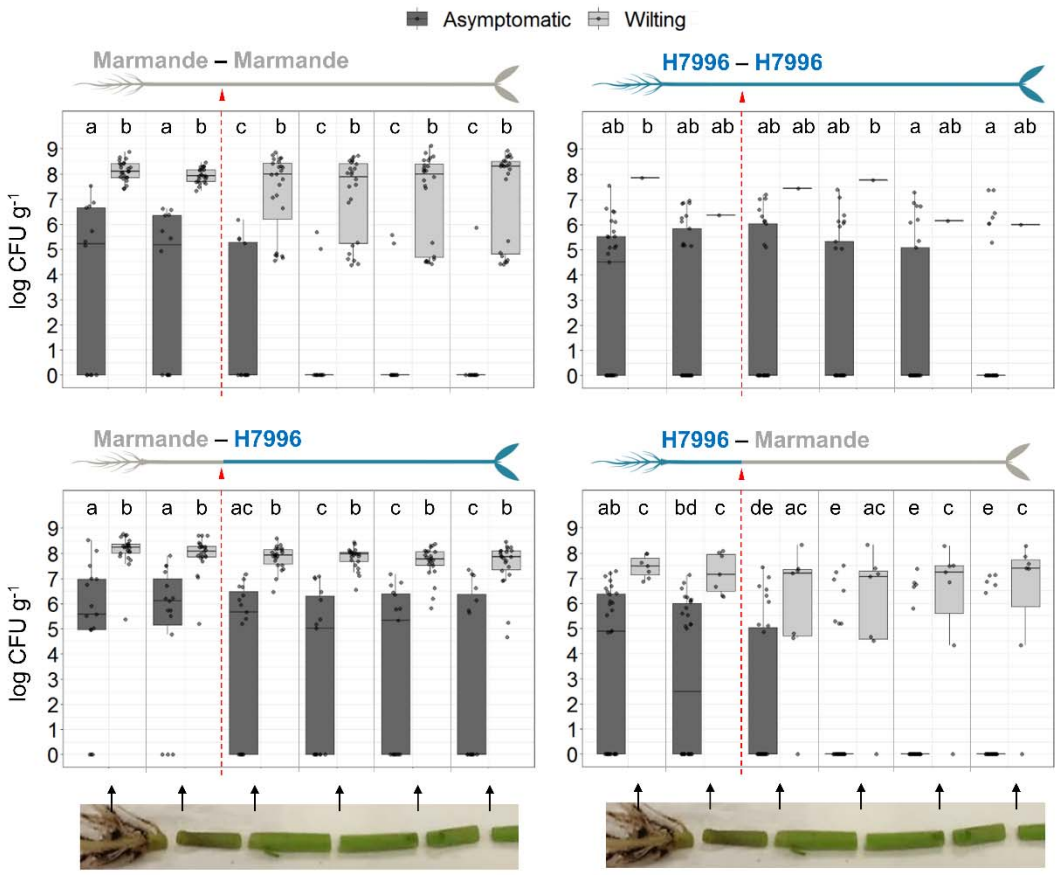
Asymptomatic
Wilting
Marmande – Marmande
H7996 – H7996
Marmande – H7996
H7996 – Marmande
log CFU g-1

Fig. 6

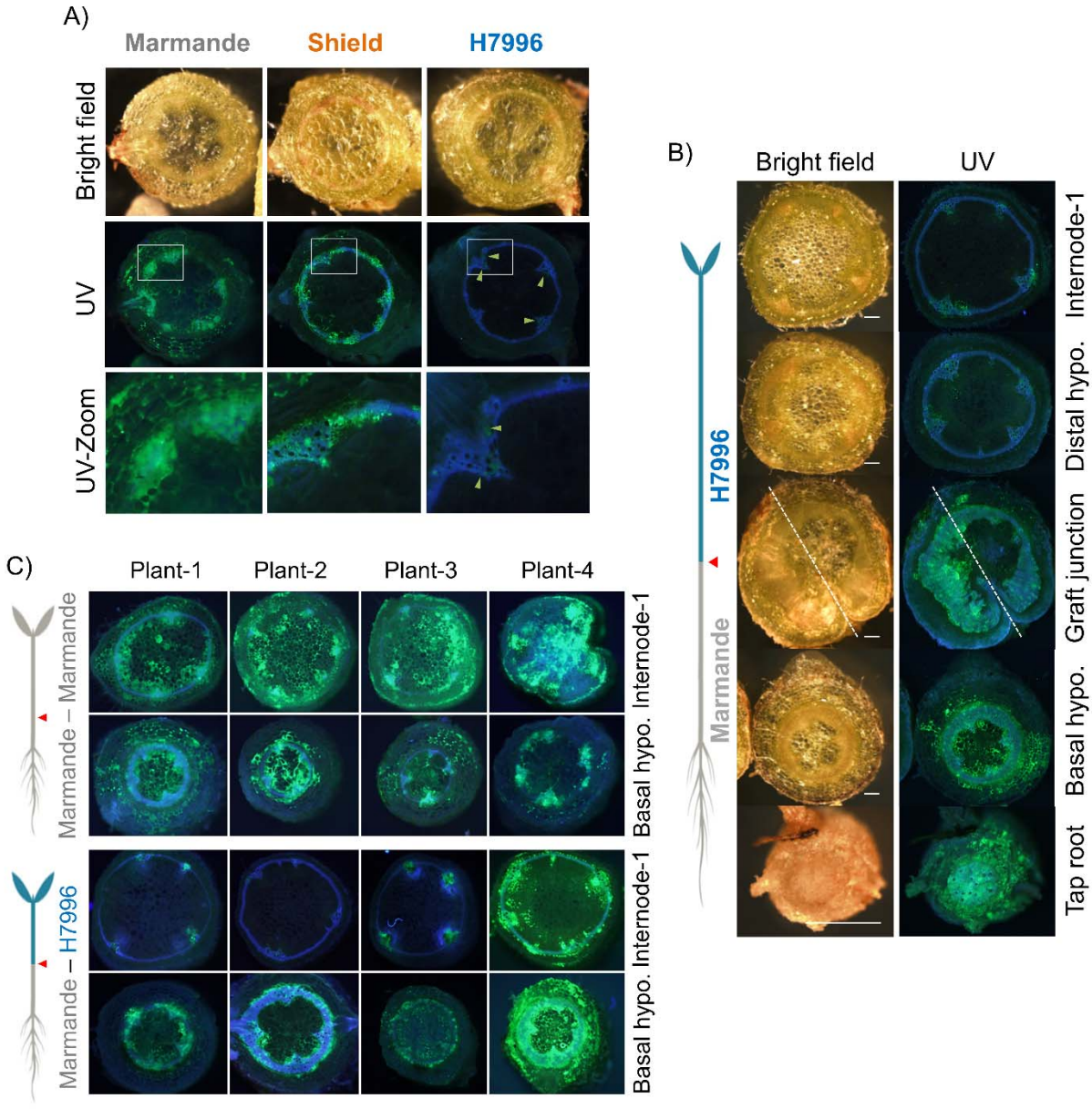
A)
Marmande
Shield
H7996
Bright field
UV
UV-Zoom
B)
Bright field
UV
H7996
Marmande
Internode-1
Distal hypo.
Graft junction
Basal hypo.
Tap root
C)
Plant-1
Plant-2
Plant-3
Plant-4
Marmande – Marmande
Basal hypo. Internode-1
Marmande – H7996
Basal hypo. Internode-1

Fig. 7

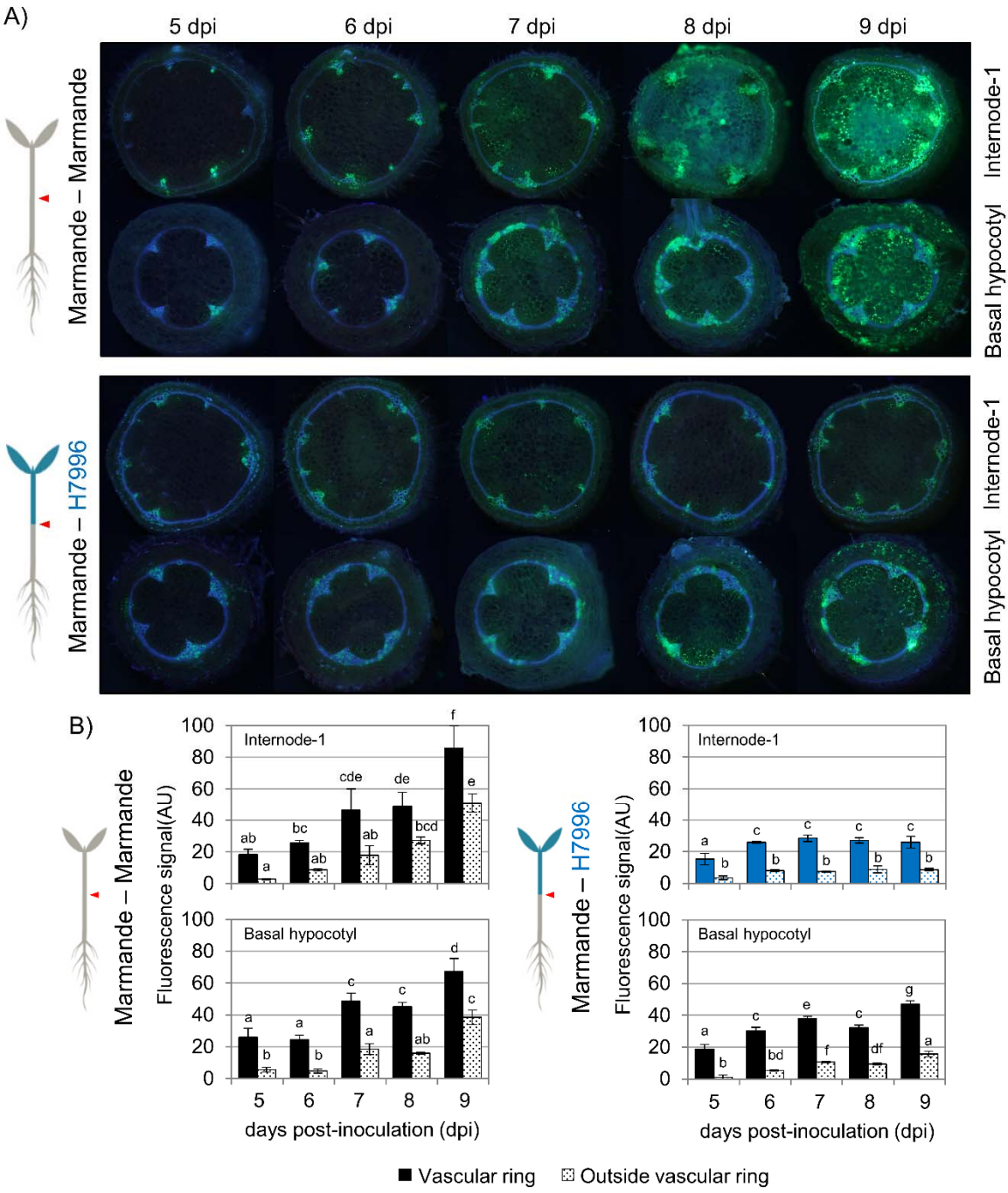
A)
5 dpi
6 dpi
7 dpi
8 dpi
9 dpi
Marmande – Marmande
Marmande – H7996
Internode-1
Basal hypocotyl
B)
Fluorescence signal(AU)
Internode-1
Basal hypocotyl
days post-inoculation (dpi)
Vascular ring
Outside vascular ring

Fig. 8

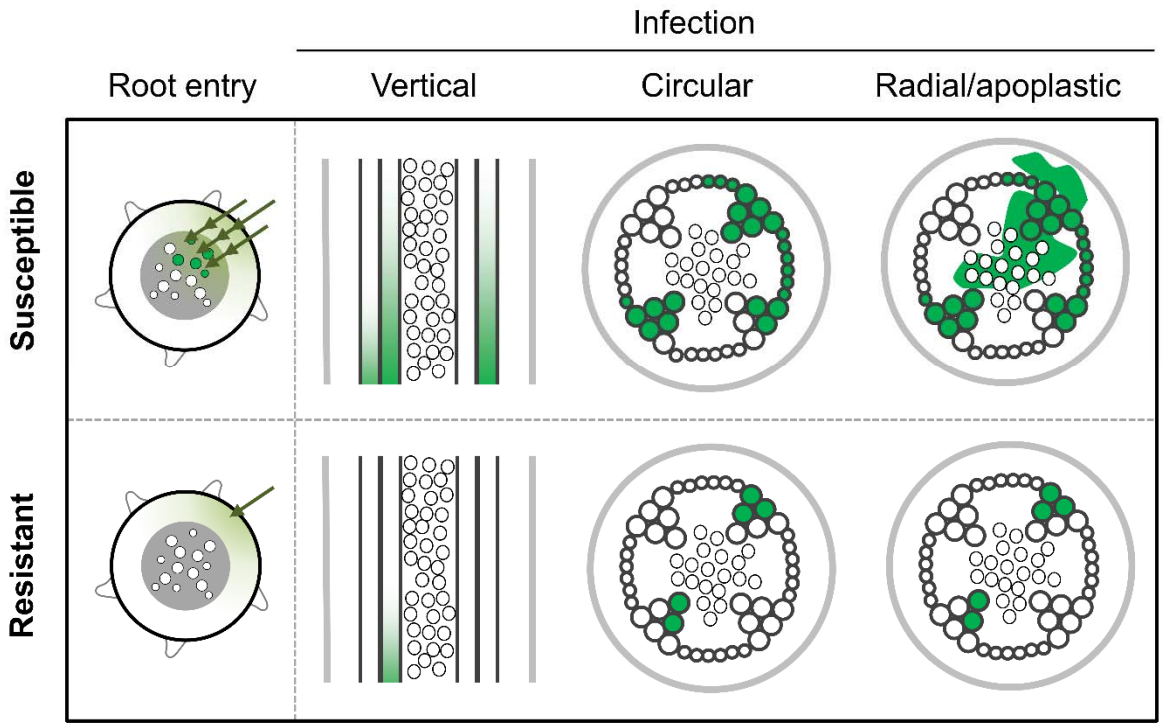
Infection
Root entry
Vertical
Circular
Radial/apoplastic
Susceptible
Resistant

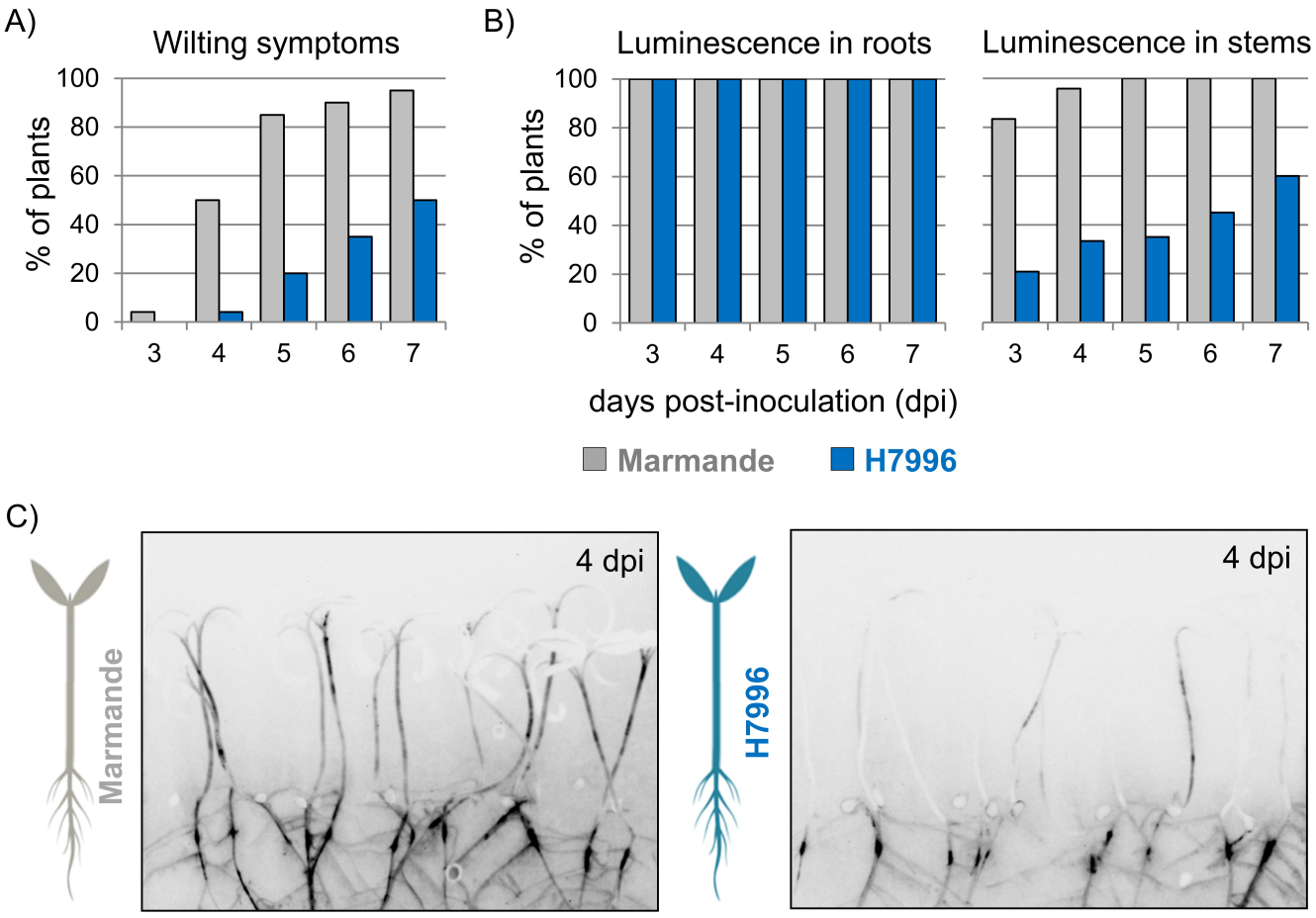
A)
Wilting symptoms
% of plants
100
80
60
40
20
0
3
4
5
6
7
B)
Luminescence in roots
Luminescence in stems
% of plants
days post-inoculation (dpi)
Marmande
H7996
C)
Marmande
4 dpi
H7996
4 dpi

A)

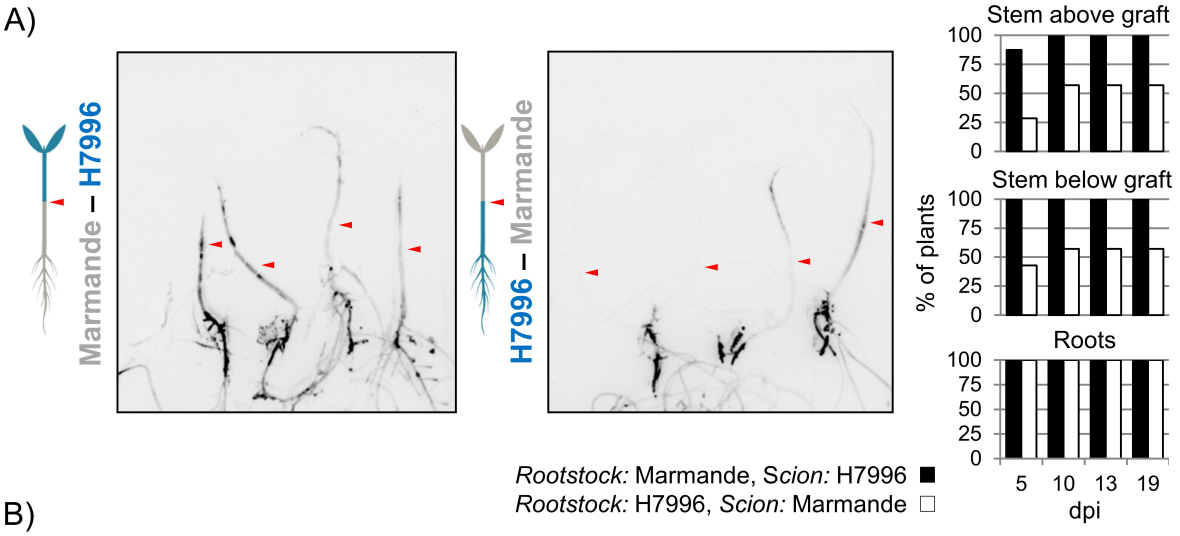
Marmande – H7996
H7996 – Marmande
Stem above graft
Stem below graft
Roots
% of plants
100
75
50
25
0
5
10
13
19
dpi
Rootstock: Marmande, Scion: H7996
Rootstock: H7996, Scion: Marmande

B)

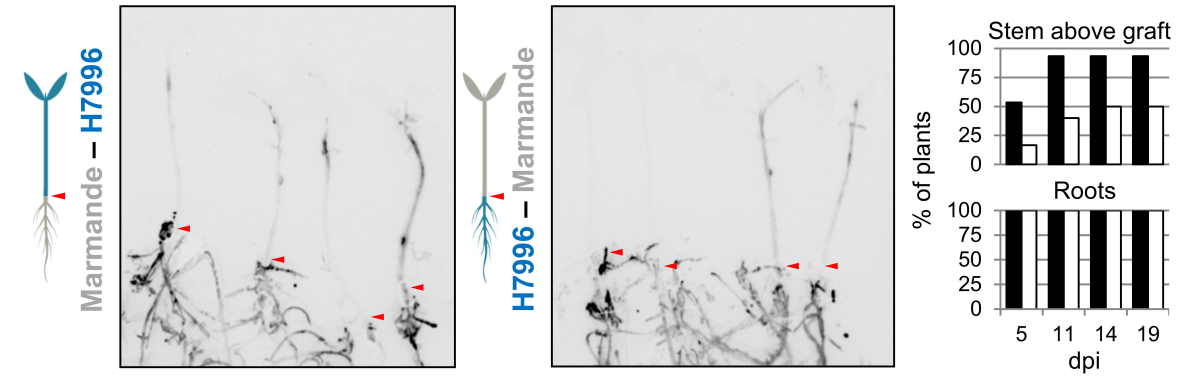
Marmande – H7996
H7996 – Marmande
Stem above graft
Roots
% of plants
100
75
50
25
0
5
11
14
19
dpi

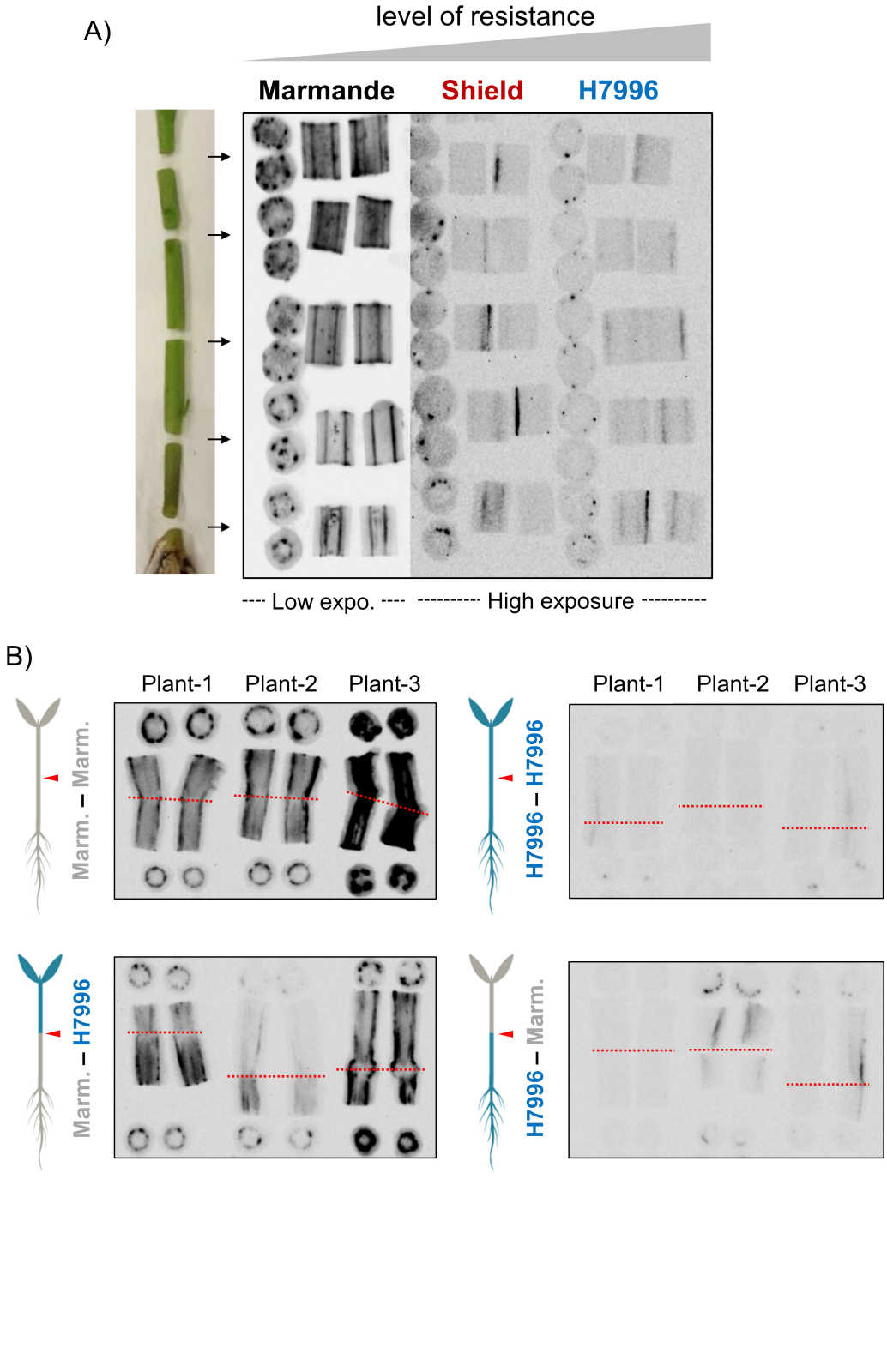
A)
level of resistance
Marmande
Shield
H7996
---- Low expo. ---- ---------- High exposure ----------
B)
Plant-1
Plant-2
Plant-3
Marm. – Marm.
H7996 – H7996
Marm. – H7996
H7996 – Marm.

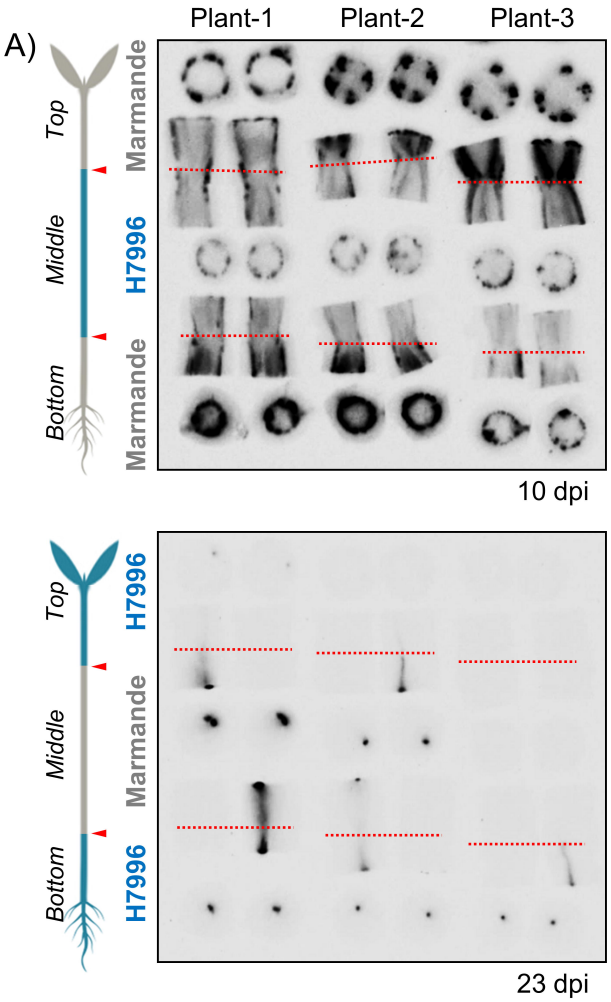
A)
Plant-1
Plant-2
Plant-3
Top
Middle
Bottom
Marmande
H7996
Marmande
10 dpi
Top
Middle
Bottom
H7996
Marmande
H7996
23 dpi

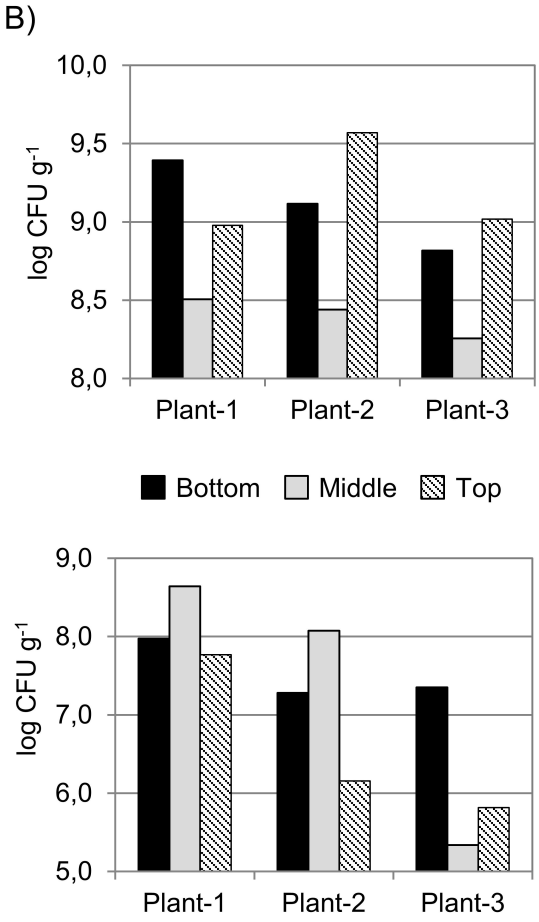
B)
10,0
9,5
9,0
8,5
8,0
log CFU g-1
Plant-1
Plant-2
Plant-3
Bottom
Middle
Top
9,0
8,0
7,0
6,0
5,0
log CFU g-1
Plant-1
Plant-2
Plant-3

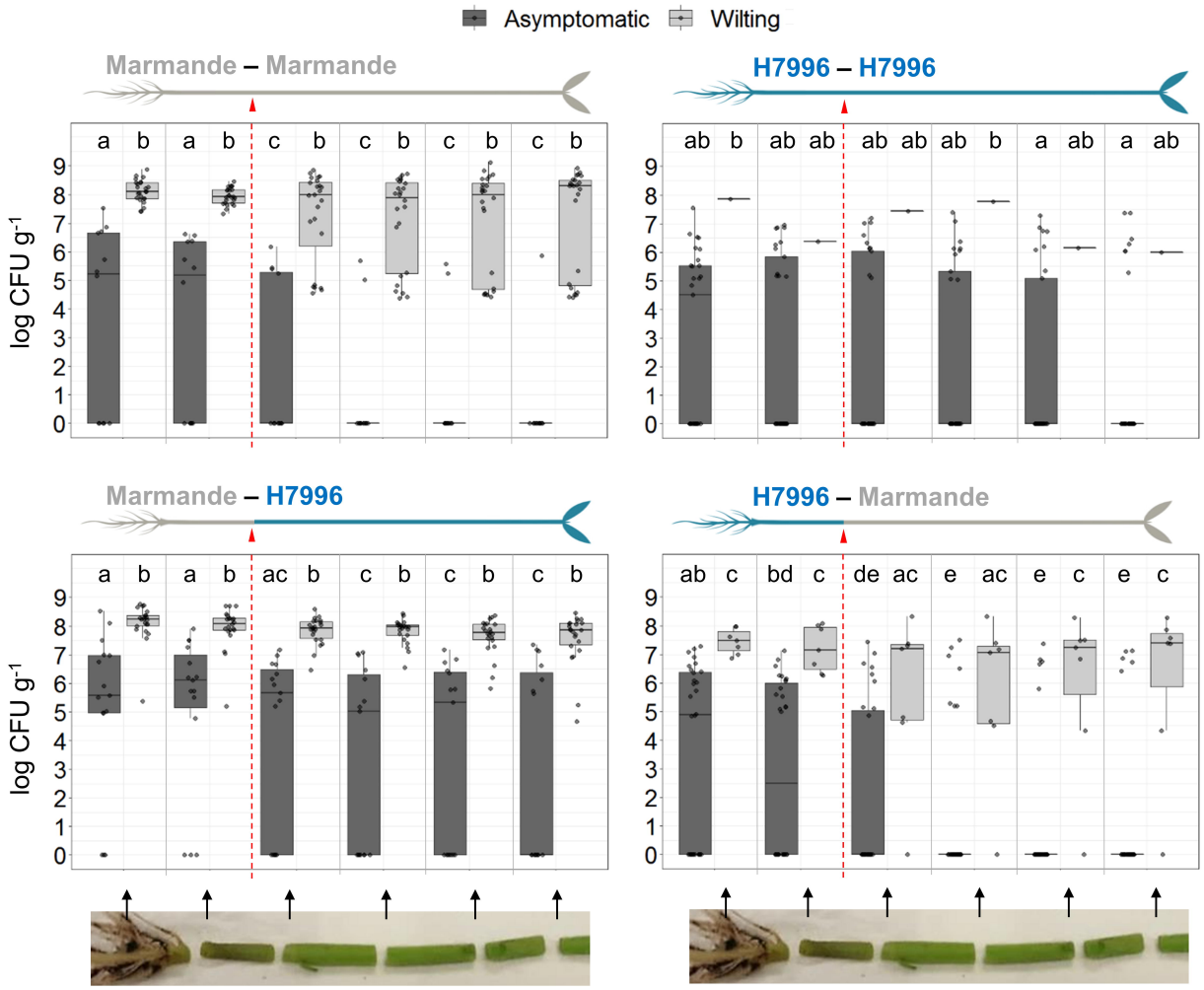
Asymptomatic
Wilting
Marmande – Marmande
H7996 – H7996
Marmande – H7996
H7996 – Marmande
log CFU g-1
a b a b c b c b c b c b
ab b ab ab ab ab ab b a ab a ab
a b a b ac b c b c b c b
ab c bd c de ac e ac e c e c
0 1 2 3 4 5 6 7 8 9

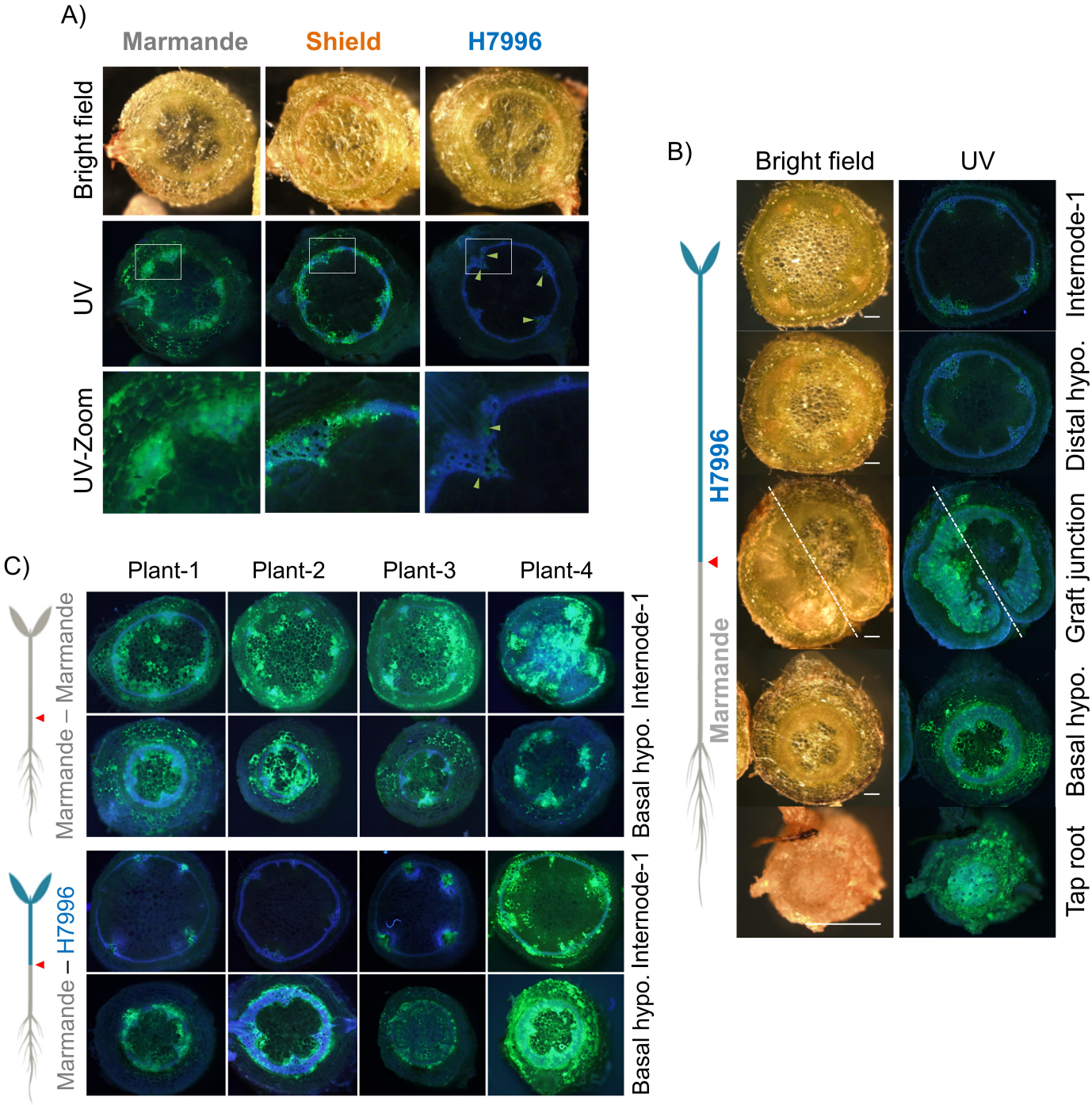
A)
Marmande
Shield
H7996
Bright field
UV
UV-Zoom
B)
Bright field
UV
H7996
Marmande
Internode-1
Distal hypo.
Graft junction
Basal hypo.
Tap root
C)
Plant-1
Plant-2
Plant-3
Plant-4
Marmande – Marmande
Marmande – H7996
Basal hypo. Internode-1
Basal hypo. Internode-1

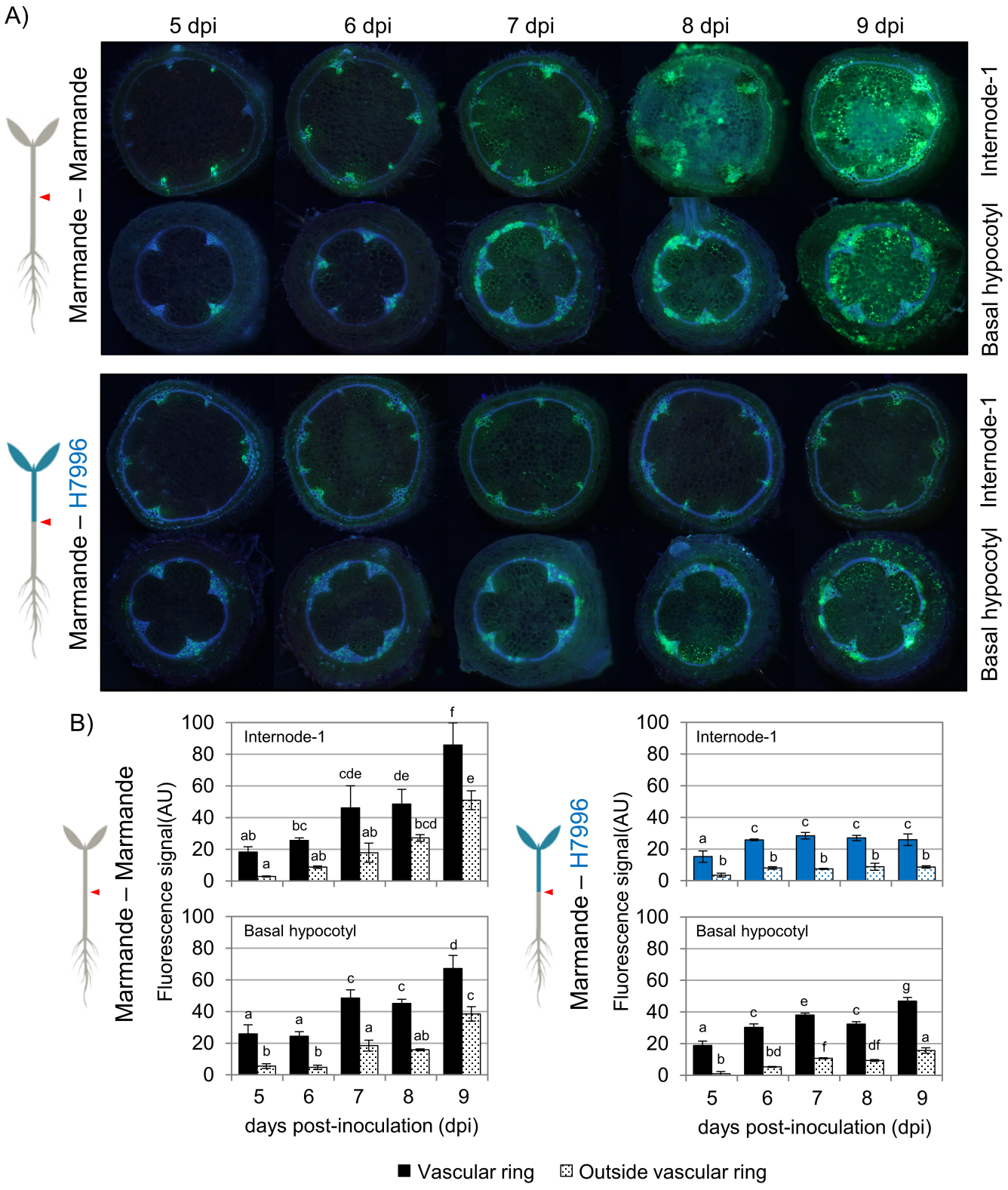
A)
5 dpi
6 dpi
7 dpi
8 dpi
9 dpi
Marmande – Marmande
Marmande – H7996
Internode-1
Basal hypocotyl
B)
Fluorescence signal(AU)
Internode-1
Basal hypocotyl
days post-inoculation (dpi)
Vascular ring
Outside vascular ring

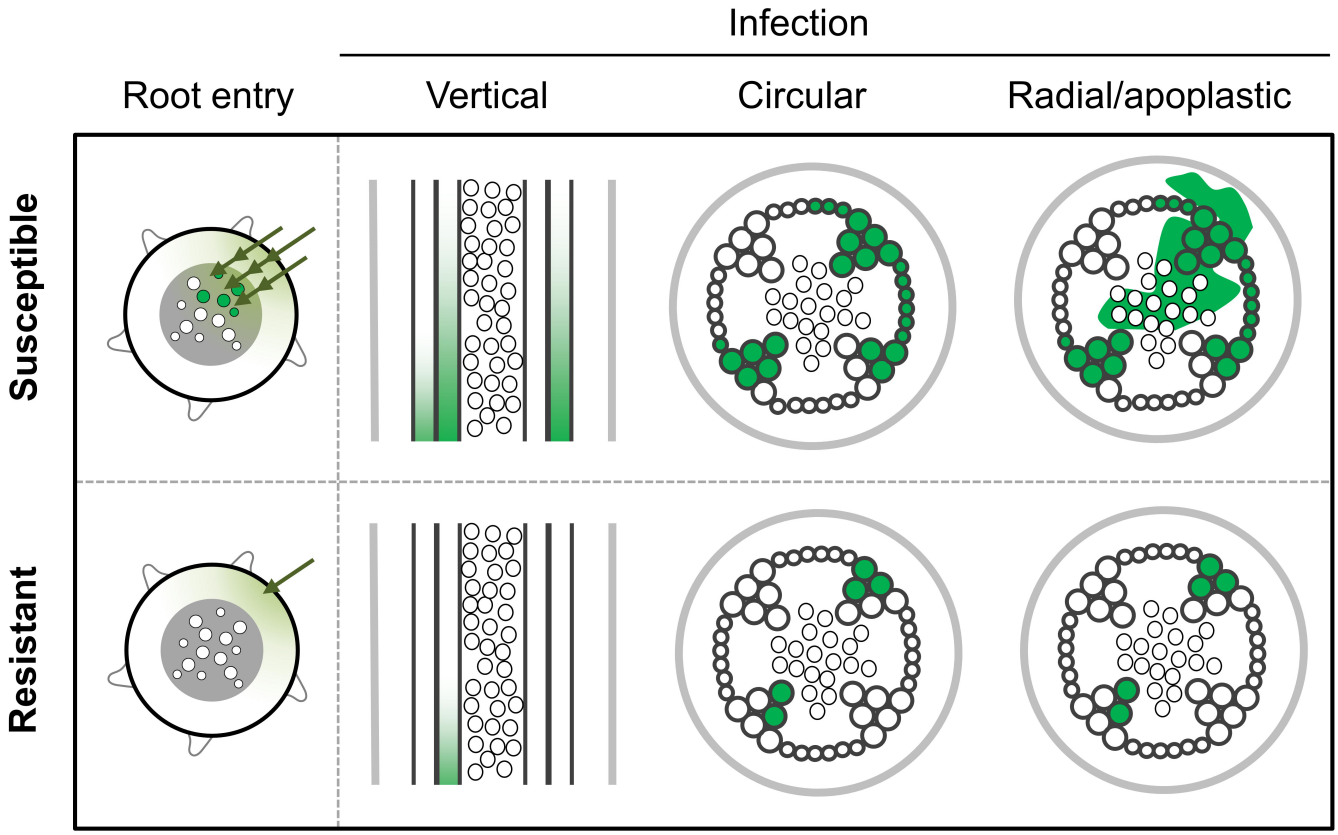
Infection
Root entry
Vertical
Circular
Radial/apoplastic
Susceptible
Resistant